Thermal Qualification Program of NASA's Multiple Payload Ejector (MPE) for Responsive Deployment of Small Satellites on a Single Launch Vehicle

A Thesis Presented to the

Aerospace Engineering Department Faculty of

California Polytechnic State University, San Luis Obispo

In Partial Fulfillment

Of the Requirements for the

Master of Science Degree in Aerospace Engineering

By

Roland Coelho

October 2012

COMMITTEE MEMBERSHIP

TITLE:	Thermal Qualification Program of NASA's Multiple Payload Ejector (MPE) for Responsive Deployment of Small Satellites on a Single Launch Vehicle
AUTHOR:	Roland Coelho
DATE SUBMITTED:	October 2012
COMMITTEE CHAIR:	Jordi Puig-Suari, PhD.
COMMITTEE MEMBER:	Kira Abercromby, PhD.
COMMITTEE MEMBER:	Eric Mehiel, PhD.
COMMITTEE MEMBER:	Gerald Shaw, PhD.

ABSTRACT

Thermal Qualification Program of NASA's Multiple Payload Ejector (MPE) for Responsive Deployment of Small Satellites on a Single Launch Vehicle

Roland Coelho

This thesis describes the passive thermal design of NASA's Multiple Payload Ejector (MPE) using optical coatings and insulation blankets, thermal analysis performed on the MPE in worst case hot and cold orbits as well as thermal vacuum chamber simulation, the results of the MPE system level qualification thermal vacuum test, and the correlation of data between the modeling analysis and the thermal vacuum test. Initial conditions, environments, and model construction are discussed along with the Thermal Desktop predictions for worst case flight conditions and thermal balance. The temperature data from the thermal vacuum test is compared with the predictions from Thermal Desktop, and the model will be updated for heat generation and conduction values if needed.

The scope of this document is limited to a "2-Stack" MPE configuration.

After analyzing the MPE thermal vacuum test data and comparing it to the thermal model, MPE demonstrates all avionics hardware to have a 20°C margin over worst case hot and cold flight predictions. Therefore from a thermal perspective, the MPE is fully qualified for flight.

ACKNOWLEDGEMENTS

Dr. Marco Villa, Robert Davis, Garrett Skrobot and NASA MPE Team —
For giving me the opportunity to be a part of your NASA MPE Team and providing me with invaluable experience in such a professional work environment. It was truly a pleasure working with all of you and hope we cross paths again in the future.

Dr. Jordi Puig-Suari, Cal Poly CubeSat PI —
For guidance and leadership to the entire Cal Poly CubeSat Program throughout the years. Thank you for all the amazing opportunities to work on CubeSat launches opportunities around the world as I slowly progressed through my thesis. I wouldn't trade this experience for anything.

Dr. Eric Mehiel, Dr. Kira Abercromby, Dr. Gerry Shaw, Thesis Committee —
For the motivation and support for me to complete my thesis and the daily reminders as I try to sneak past your offices.

CubeSat and PolySat Teams —
For being part of my family over the past decade. It's been truly an honor to work with all of you. Surprisingly I am not the last person of my generation to finish my thesis, so Kyle Leveque, tag you're it!

Melody Golobic —
For being the main driver in motivating me to complete my thesis. I would be in the same position now as I was a year ago if it wasn't for you.

My Family —
Thanks for soo many years of unquestioned love and support.

TABLE OF CONTENTS

LIST OF TABLES

LIST OF FIGURES

1. MULTIPLE PAYLOAD EJECTOR INTRODUCTION

1.1 SCOPE

This document describes the passive thermal design of the Multiple Payload Ejector (MPE) using optical coatings and insulation blankets, thermal analysis performed on the MPE in worst case hot and cold orbits as well as thermal vacuum chamber simulation, the results of the MPE system level qualification thermal vacuum test, and the correlation of data between the modeling analysis and the thermal vacuum test. Assumptions, environments, and model construction will be discussed along with the Thermal Desktop predictions for worst case flight conditions, thermal balance, and thermal cycle temperatures. The temperature data from the thermal vacuum test will be compared with the predictions from Thermal Desktop, and the model will be updated for heat generation and conduction values if needed.

The scope of this document is limited to a "2-Stack" MPE configuration.

After analyzing the MPE thermal vacuum test data and comparing it to the thermal model, MPE demonstrates all avionics hardware to have a 20°C margin over worst case hot and cold flight predictions. Therefore from a thermal analysis perspective, the MPE is fully qualified for flight.

1.2 PROJECT DESCRIPTION

The Multiple Payload Ejector (MPE) is a modular small spacecraft carrier designed to fly on a DARPA Falcon class launch vehicle (LV). The intent is to provide low-cost access to space for educational- and small-satellite-class experiments. The MPE consists of a flat plate top, and one or two segments resembling an I-beam on which to mount small

spacecraft and their separation systems. These configurations can support a primary payload plus 2 or 4 secondary payloads, and potentially multiple tertiary payloads with their ejection systems.

The MPE is designed to switch on following receipt of a launch vehicle's separation signal. Once powered on, the MPE then proceeds to actuate payload separation systems in a pre-determined sequence while telemetering the state of the MPE's systems through the Tracking Data Relay Satellite System (TDRSS) Space Network.

MPE avionics consist of battery charge electronics for payload battery charging prior to launch, a timer and separation circuitry to eject payloads, a telemetry system to provide confirmation of payload separation, and an input conditioning circuit to receive the LV's separation signal and enable the timer, separation circuitry, and telemetry subsystem.

2. ABBREVIATIONS AND ACRONYMS

CCMS	Centralized Configuration Management System
CM	Configuration Management
CO	Chamber Operator
CPT	Comprehensive Performance Test
CVCM	Collected Volatile Condensable Materials
DARPA	Defense Advanced Research Projects Agency
EGSE	Electrical Ground Support Equipment
ESD	Electrostatic Discharge Control
FTD	Functional Test Director
GEVS	General Environmental Verification Specification
GSFC	Goddard Space Flight Center
GSE	Ground Support Equipment
I&T	Integration and Test
ICD	Interface Control Document
IMT	Integrated Management Team
IR	Infrared
LCT2	Low Cost TDRSS Transceiver
LCTE	Low Cost Telemetry Encoder

LEO	Low Earth Orbit
LPT	Limited Performance Test
LV	Launch Vehicle
MLB	Motorized Lightband
MLI	Multi-Layered Insulation
MPE	Multiple Payload Ejector
NASA	National Aeronautics and Space Administration
PDL	Product Design Lead
P-POD	Poly Picosatellite Orbital Deployer
PSC	Planetary Systems Corporation
RF	Radio Frequency
RPMT	Remotely Programmable Multifunction Timer
RTD	Resistance Temperature Detector
TDRSS	Tracking Data Relay Satellite System
TD	Test Director
TML	Total Mass Loss
TTE	Thermal Test Engineer
TTD	Thermal Test Director
VDA	Vapor-Deposited Aluminum

WFF	Wallops Flight Facility

3. MPE SYSTEM LEVEL DESIGN

3.1 DEFINITION OF ALL REQUIREMENTS

These requirements are derived at the MPE system level to ensure a successful flight of MPE and are flowed down to the thermal discipline for verification. There are also general mission level objectives for the thermal system, however it is not formally tracked in requirement verifications.

3.1.1 System Level Requirements

– 1.0 – MPE shall accommodate multiple payloads (and their ejection systems).

– 1.4 – MPE shall be modular to support different configurations of payloads.

– 1.5 – MPE shall be designed for simultaneous integration of payloads.

– 1.6 – MPE shall not harm or degrade payloads.

– 1.6.2.5 – A thermal materials list shall be maintained.

– 1.6.2.6 – Thermal components and margins shall have TML < 1% and CVCM < 0.1% using NASA Ref Pub 1124, “Outgassing Data for Spacecraft Materials”.

– 2.0 – MPE shall be compatible with the launch vehicle.

– 2.1 – MPE shall be designed and tested per GEVS.

– 2.2 – MPE shall be compatible with typical launch vehicle environments.

– 2.2.5.1 – MPE avionics shall perform over temperature range per TBD document.

– 2.3 – MPE shall be compatible with the launch vehicle.

– 2.6 – MPE shall vent internal MPE volumes at a rate consistent with ascent

requirements.

– 2.7 – MPE shall be compatible with typical launch pad environments.

– 3.4 – MPE shall be compatible with identified payloads:

–Starshine, CX-1

– 3.7 – MPE shall be manifested to three segments high or less.

– 5.0 – MPE shall be designed using standard engineering practices.

– 7.0 – MPE shall be flight ready on budget:

– Mass, power, money, schedule etc.

– 7.7 – MPE shall maintain adequate thermal margins.

– 7.7.1 – MPE shall be ready for payload integration within allocated thermal margins.

– 7.7.2 – Scheduled reviews shall track thermal margins.

– 7.7.3 – Thermal margin shall be estimated and tracked.

– Protoflight units must be designed with 15°C margin (5°C modeling uncertainty, 10°C testing) over duration of mission.

– Source: GEVS-STD-7000, GSFC-STD-1000

3.1.2 Overall Mission Objectives

– Maintain MPE avionics boxes with 15°C margins to manufacturer's operational limits over one orbit (requirement).

– 5°C analytical uncertainty, 10°C qualification above and beyond that for testing proto-flight units.

– Passive Thermal Design

    – No budget for heater power

– Strategy for Accommodating Payloads

– Perform integrated analysis on manifest

– Timer limits duration of “active” portion of mission to 54 minutes

– Cold case (2-impulse insertion) effects:

    – Coast inactive for ~45 minutes while in transfer orbit

    – MPE activated at MECO2, on for 54 minutes

    – Total survival time: ~99 minutes (>1 orbit)

– Hot case (1-impulse insertion) effects:

    – MPE activated at MECO1, on for 54 minutes

    – Total survival time: 54 minutes

4. MPE ANALYTICAL MODEL

4.1 DEFINITION OF WORST CASE ASSUMPTIONS

4.1.1 Worst Case Cold Orbit

MPE must operate nominally in the worst case cold conditions in the event ideal launch and orbit conditions cannot be obtained from the launch vehicle. The MPE operational duration requirement is 54 minutes, which is driven by the Timer box and the power capacity of the onboard batteries. The worst case cold scenario assumes a dual impulse insertion by the launch vehicle. The first impulse would be a transfer orbit which would last approximately 45 minutes at which MPE will be in an inactive state and no avionics will be operating. At the start of the second impulse into the final orbit, the launch vehicle will send a deployment signal to the MPE. This deployment signal will start the timer and MPE will be active for 54 minutes while it delivers all of its payloads into orbit. The MPE orientation for the inactive portion of the flight will have the launch vehicle adapter ring facing the nadir direction, and once the separation signal is sent, MPE will be deployed from the upper stage of the launch vehicle and the primary spacecraft will be in line with the solar vector. This orientation was chosen to minimize the amount of incident solar flux, Earth IR, and albedo on MPE.

The Figure 1 shows the worst case cold orbit.

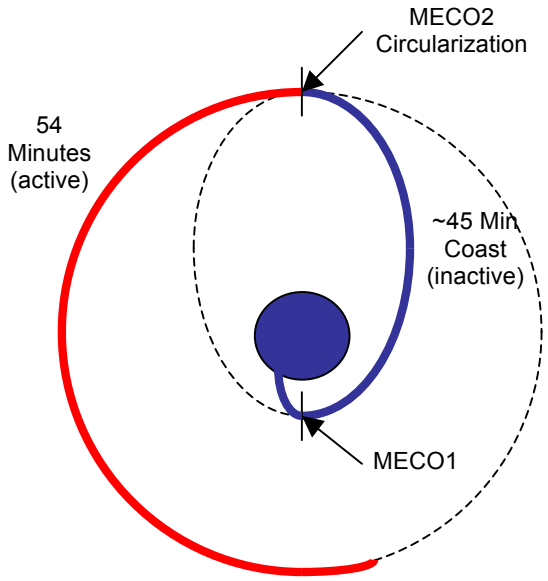

Figure 1 - Worst Case Cold 2-Impulse Orbit

4.1.2 Worst Case Hot Orbit

MPE must operate nominally in the worst case hot conditions in case of less than ideal orbit and launch conditions. The time duration and operations for the worst case cold orbit are also valid for the hot case. The MPE orientation for both the inactive and active portion of the flight will have the avionics flange always facing the solar vector, and once the separation signal is sent, MPE will remain attached to the upper stage of the launch vehicle and the primary spacecraft will be in line with the velocity vector. This orientation was chosen to maximize the amount of incident solar flux, Earth IR, and albedo on MPE. An identical worst case hot orbit will be simulated for the opposite side avionics flange.

Figure 2 is an illustration of the worst case hot orbit. Initially, the worst case hot orbit assumed a single impulse to orbit as in the left illustration. After further analysis, the dual impulse insertion provided added heat flux to the avionics during the inactive coast.

The difference in temperatures from the single and dual impulse will be shown in the orbital temperature predictions.

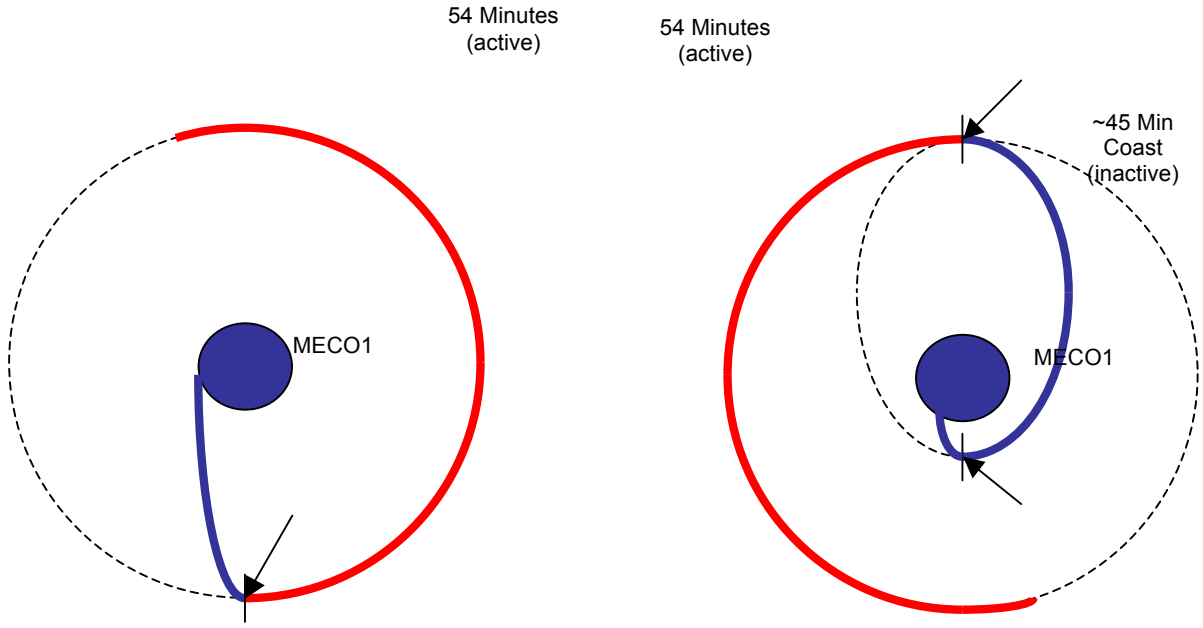

Figure 2 - Previous Single Impulse Hot Case and Current Dual Impulse Hot Case

4.1.3 Worst Case Environment Assumptions

Table 1 shows the assumptions used for the worst case hot and cold environments in the Thermal Desktop model. The major differences include the launch site, the initial model temperatures, and the avionics power generation. The hot case would launch out of Vandenberg Air Force Base, with a beta angle of 90° and an initial MPE temperature of 30°C. The avionics power generation was increased by 10% for added margin. The cold case would launch out of Wallops Flight Facility, with a beta angle of 0° and an initial MPE temperature of 10°C. The avionics power generation was decreased by 10% for added margin.

Table 1 - Thermal Environment Assumptions

	Cold Case	Hot Case
Launch Site	WI	VAFB
Orbit Altitude	350 km	350 km
Orbit Inclination	35°	66.6°
Beta Angle	0°	90°
Free Molecular Heating	None	None
Solar Constant	1286 W/m^2	1419 W/m^2
Albedo	25% of direct solar	35% of direct solar
Earth IR	208 W/m^2	265 W/m^2
Ascent Case	Neglected	Neglected
Liftoff Temperature	10°C	30°C
Power State	Off for first half of orbit, on for 2nd half of orbit (2-impulse insertion)	Off for first half of orbit, on for 2nd half of orbit (2-impulse insertion)
Orientations Considered	Inertial drift, base blocking sun	Inertial Drift: (1) +Z (Telem) side facing sun (2) -Z (Misc) side facing sun
LV Attachment State	Attached through lightband first half of orbit, free-flying 2nd half of orbit	Bolted directly to LV
Soakback	Not considered (LV stays at initial temperature	Peaks to 150°C after 175s, drifts linearly to -32C at 99 min
Mass Multiplier	0.9	0.9
Power Multiplier	0.9	1.1

4.1.4 Prelaunch Environments

Prelaunch environments were derived from typical launch environments for DARPA Falcon class launch vehicles (SpaceX Falcon 1 or Orbital Sciences Minotaur launch vehicles) and typical small to medium class launch vehicles. Since MPE will occupy the primary payload volume in the fairing, prelaunch environments are well controlled. Conditioned air is constantly flowing in the primary payload volume from the time of MPE integration to the launch vehicle upper stage through launch. Since this

environment is well controlled at an average of 20°C, a tolerance of ±10°C was used for the worst case hot and cold prelaunch environments.

4.1.5 Possible Max. Solar and Eclipse Orbits

Solar flux, Albedo, and Earth IR values were acquired from Spacecraft Thermal Control Handbook, Volume 1: Fundamental Technologies by David G. Gilmore. A margin of 10% was used for both the hot and cold case, increasing and reducing these radiation environments accordingly.

4.1.6 Heat Generation of MPE Components

An estimate of the thermal heat generated is derived from actual power readings during a Comprehensive Performance Test for most of the avionics, which exercises all MPE avionics in flight configuration. The lead electrical engineer for MPE provided the power draw readings and a worst case estimate of power converted into waste heat. However, there are several boxes like the MPE and Initiator Battery Boxes where power could not be measured. Worst case analysis was performed to calculate the maximum amount of heat the batteries would generate given the stored capacity, the power efficiency, the expansion properties, and the remainder as heat generated.

Table 2 shows the estimated thermal heat generated for the cold and hot cases, as well as a 10% increase for the hot case and a 10% decrease for the cold case.

Table 2 - Avionics Power Margins

Avionics Power Dissipation (2-Stack) with Realistic Payloads

	Cold			Hot		
Item	Actual Power	Margin	Model Power Input	Actual Power	Margin	Model Power Input
Timer	0.84	0.9	0.76	0.84	1.1	0.92
LCT2 Transmitter	45	0.9	40.50	45	1.1	49.50
LCTE	4.8	0.9	4.32	4.8	1.1	5.28
Telemetry Monitor	0.51	0.9	0.46	0.51	1.1	0.56
MPE Battery	0.0	0.9	0.0	15.5	1.1	17.05
Initiator Battery	0.65	0.9	0.59	0.65	1.1	0.72
Rate Sensors	1.2	0.9	1.08	1.2	1.1	1.32
Battery Charge Box	0	0.9	0.00	0	1.1	0.00
Battery Monitor Box	0	0.9	0.00	0	1.1	0.00
Power Output Box	0	0.9	0.00	2.2	1.1	2.42
Relay Box	4.61	0.9	4.15	4.61	1.1	5.07
Splitter	0	0.9	0.00	0	1.1	0.00
Total	57.61	0.9	51.85	75.31	1.1	82.84

4.2 DESIGNING THE THERMAL MODEL

4.2.1 Thermal Desktop Model Construction

The structural members of the MPE were constructed using the finite difference solid functions in Thermal Desktop in two flight configuration segments. Each MPE segment was modeled as six parts: two 24”x22”x1” isogrid “web” halves, two 30”x22”x1” isogrid “flange” pieces mounted orthogonally to the web halves, and two 30”x22”x1/8” cover plates for the isogrid “flanges.” The primary plate was constructed as a 26”x30”x1.5” isogrid aluminum panel with a 15” bolt circle for mounting the primary payload’s separation mechanism. The isogrid half of the primary plate is closed with a 1/8” aluminum cover plate. If the primary payload is sufficiently massive, a second identical plate may be added and the cover plate eliminated. The gussets are modeled as two

6”x22”x1.5” cropped right triangular isogrid structural elements employed to increase the lateral stiffness of the MPE. The antenna standoffs are modeled as rectangular posts between the antennas and the main structure, improving the antenna’s coverage. The LV adapter flange is the base plate for the MPE. This flange enables the MPE structure to mount to either the launch vehicle or the launch vehicle’s separation system. The baseline assumes a bolt pattern consistent with that of Planetary Systems Corporation’s 38” Motorized Lightband.

All of the avionics boxes were constructed in the same manner. The Low Cost TDRSS Transmitter is modeled as a 4”x5”x1.438” box with a 4”x5” footprint that inputs 28V, outputs 10W RF, and dissipates 45W as heat. The Low Cost Telemetry Encoder is modeled as a 3.75”x4.75”x1.9” box with a 3.75”x4.75” footprint that can accept +10 to +36V (+24V nominal for MPE) and dissipates 7 W as heat. The Telemetry Monitor Box is modeled as a 3”x5”x1” box with a 3”x5” footprint. The Seavey Engineering antennas are patch antennas with an omni-directional gain pattern. Each antenna is 4”x4”x0.25” with a 4”x4” footprint and attaches to the antenna ground plane. The antenna ground planes help reduce interference effects between the two omni-directional antennas. The ground planes are 6.5” in diameter and fabricated out of FR-4 with 1 oz. /ft^2 copper, which are modeled as finite difference cylinders. The ejection timer is the NSROC Remotely Programmable Multifunction Timer (RPMT). This controls the sequence of payload ejections from the MPE. The unit is modeled as a 4”x3”x1 1/8” box with a 4”x3” footprint. All avionics boxes have 10 mil Graftech Grafoil Class 1210A thermal interface material which is modeled as the contact conductance between the avionics boxes and the segment flange covers.

The heat generated by the avionics boxes is modeled with heat loads that are applied to the finite difference blocks. The heat generation is also set on a timer, with no heat generation for the 45 minute inactive coast, and turns on at the start of the 54 minute active portion of the launch.

4.2.2 Flight Thermal Design

The MPE flight thermal design is a passive hot biased design. Multi-Layer Insulation (MLI) blankets cover most of the avionics situated on the flange covers. These MLI blankets consist of 15 layers, with 2 mil second surface Vapor- Deposited Aluminum (VDA) Kapton outer layers, 0.25 mil aluminized Mylar inner layers, and B2A Dacron netting separating each layer. The MLI blankets are also used in the web interfaces to shield payloads from each other, and also in the launch vehicle adapter ring to minimize launch vehicle soakback. Instead of physically modeling the MLI as a component, the built-in insulation/MLI feature is used in Thermal Desktop. The MLI is modeled as an arithmetic node layer offset from the surface of the specified components. An effective emissivity value of 0.05 was used for all the blankets. This feature was used to cover the upper and lower flange covers, all the avionics with the exception of the LCT2, LCTE, and the LCT Doubler, and the area inside the web openings and launch vehicle adapter ring.

The LCT2 and the LCTE generate the most of the avionics' heat, so these two components are placed on a 3/8" thick aluminum plate to act as a doubler. This area becomes an effective radiator with the use of 10 mil silver Teflon tape, with a solar absorbtivity of 0.09 and an IR emissivity value of 0.88. The silver Teflon tape is placed on all non-mating outward surfaces of this radiator. 10 mil silver Teflon tape is also

applied to the outboard surface of the antenna ground plane. This prevents the antenna from over-heating due to external heat sources during the mission, as MLI is not possible to shield the antenna. The 10 mil silver Teflon tape is modeled using the Radiation function to assign the proper optical surface properties to the LCT radiator and the antenna ground plane.

The secondary payload volume and the primary plate will be covered with a two tape scheme, using 80% first surface 1 mil VDA Kapton tape and 20% second surface 2mil VDA Kapton tape. A solar absorbtivity and IR emissivity of 0.17 help prevent excessive cooling or overheating of the structure. This is implemented in a similar fashion as the silver Teflon tape using the Radiation function and the specular surface set to these values.

Figure 3 depicts the thermal coatings and hardware from the Thermal Desktop model.

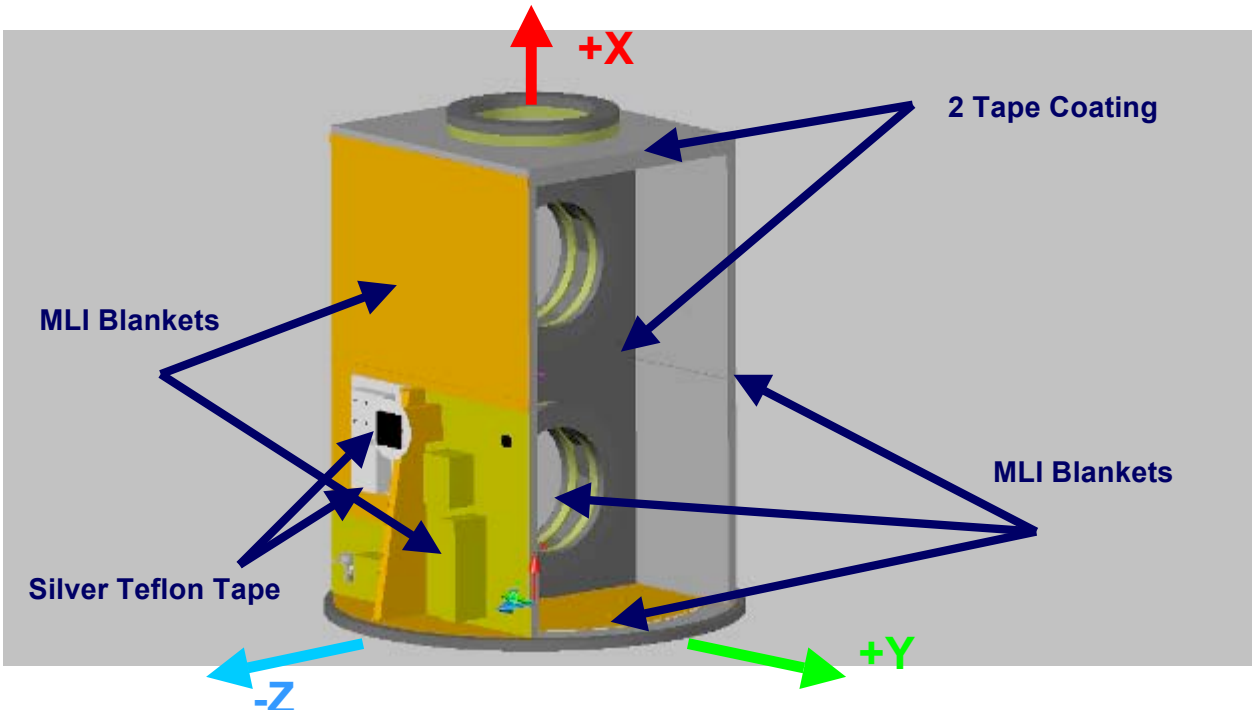

Figure 3 - Modeled Thermal Surfaces Using Thermal Desktop

4.2.3 Separation Systems

4.2.3.1 15" Motorized Lightband

The 15" Motorized Lightband (MLB) is the separation system planned for MPE. The MLBs are located on either side of the assembled web and on the primary plate.

The 15" MLBs are modeled as two halves in an attempt to realistically predict temperatures of each of the halves. PSC advertises a conductance of 0.209 ºC/W resistance across the Lightband per PSC document 2000562, "Lightband Thermal Resistance Test." Figure 4 illustrates how the interface resistances used in the model were determined.

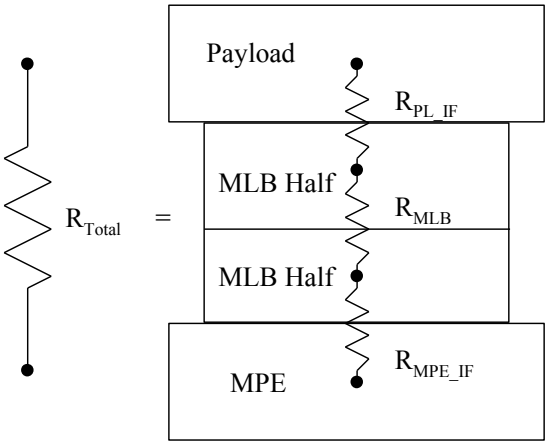

Nomenclature

R_{PL_IF} , R_{MPE_IF} – Interface resistance between MLB and payload/MPE (e.g. 24X ¼-28 bolts)

R_{MLB} – Motorized Lightband resistance

R_{MPE_IF} – Interface resistance between MLB and MPE

$$R_{PL\_IF} + R_{MLB} + R_{MPE\_IF} = R_{Total}$$

PSC advertises an R_{Total} of 0.209 °C/W for the 15" MLB, but does not break the R_{Total} into components.

Assumptions:

•R_{PL_IF} , R_{MPE_IF} is calculated from standard bolted joint resistance values: 0.5 °C/W / 24 bolts = 0.02 °C/W

•Using PSC's R_{Total} value, this implies R_{MLB} = 0.17 °C/W

Figure 4 - Lightband Thermal Resistance Values

The conductance values used within the model were determined by taking the inverse of the above resistance values. They were assigned as contact conductance on the appropriate faces of the solids.

4.2.3.2 38” Motorized Lightband

While it is preferred that the MPE remain attached, and even more preferably bolted directly to the LV without the Lightband, the possibility exists that the LV may require separation of the MPE. Currently, the 38” MLB is assumed to be the standard interface to the LV, although this must be determined prior to flight.

The worst-case hot scenario assumes attachment directly to the LV without the presence of a 38” Lightband.

The worst-case cold scenario assumes the MPE is attached to the LV via a 38” MLB up through MECO2, where the MPE is separated from the LV and free-flying for the remaining 54 minutes of the mission. The model exhibits the ability to easily change between attached and unattached states.

4.2.4 Coordinate System

The MPE coordinate system shown in Figure 5 is right-handed, with the X-axis in line with the thrust axis of the launch vehicle. The Y-axis is coincident with the secondary payloads, and the Z-axis is normal to the flange cover plates to which the avionics are mounted. The +Z avionics flange consists of an omni-directional antenna, Enable Relay Box, Initiator Battery Box, Power Out Box, and a Timer Box. The –Z avionics flange consists of an identical omni-directional antenna, Battery Charge and Monitor Box, Low Cost TDRSS Transceiver (LCT2), Low Cost Telemetry Encoder (LCTE), MPE Battery Box, Rate Sensors, and Telemetry Box.

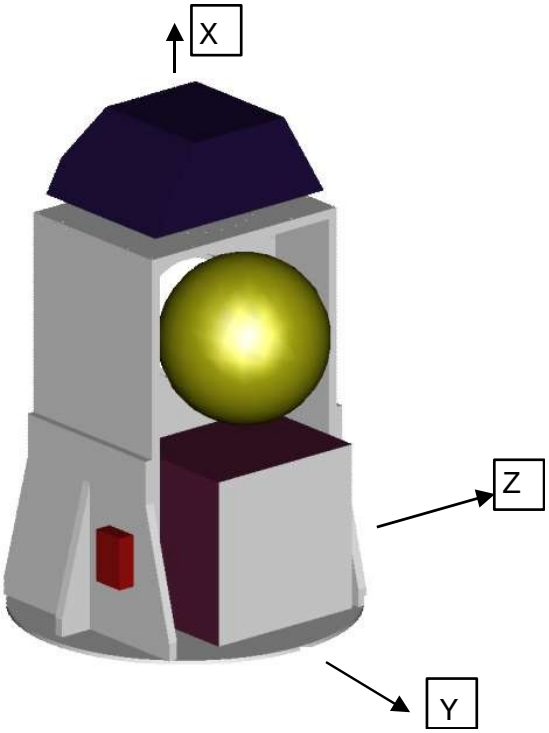

Figure 5: MPE Coordinate System

4.3 CURRENT FLIGHT PREDICTIONS

The 2-Stack MPE model yielded the following results below in

Table 3. The temperatures in the third column are the final temperatures at the end of the 99 minute flight. The temperatures in parentheses were at the time of the Critical Design Review. Changes to the orbit orientation, environment assumptions, and more accurate power dissipation numbers reflect the differences in the flight predictions at the Critical Design Review and then at the Pre-Environmental Review.

Table 3 - Flight Temperature Predictions

All Temperatures (2-Stack) with Realistic Payloads

		Cold (Start Temp = 10°C)					Hot (Start Temp = 30°C)			
Item		Operating Limit (°C)	Design Limit (°C)	Flight Prediction (°C)	Margin to Design Limit (°C)		Operating Limit (°C)	Design Limit (°C)	Flight Prediction (°C)	Margin to Design Limit (°C)
Timer		-20	-5	6.6 (8)	11.6		60	45	37.9 (41.8)	7.1
LCT2 Transmitter		-24	-9	3.9 (7.1)	12.9		65	50	46.7 (47.2)	3.3
LCTE		-20	-5	3.8 (6.5)	8.8		75	60	44.3 (45.3)	15.7
Telemetry Monitor		-20	-5	4.3 (8)	9.3		85	70	36.8 (42.6)	33.2
MPE Battery		-20	-5	6.8 (3.8)	11.8		60	45	37.2 (39.2)	7.8
Initiator Battery		-20	-5	5.2 (7.2)	10.2		60	45	37.5 (38.7)	7.5
Rate Sensors		-40	-25	4.1 (33.1)	29.1		80	65	40.8 (60.8)	24.2
Battery Charge Box		-	-	5.9 (7.4)	-		-	-	35.9 (41.5)	-
Battery Monitor Box		-	-	5.9 (7.7)	-		-	-	36.0 (40.6)	-
Power Output Box		-30	-15	6.6 (3.8)	21.6		80	65	43.5 (38.9)	21.5
Relay Box		-65	-50	5.5 (6.7)	55.5		125	110	37.0 (38.8)	73
Antennas		-100	-85	-36.6 (-49.1)	48.4		121	106	53 (79.3)	53
Splitter		-55	-40	5.6 (7.3)	45.6		85	70	34.8 (39)	35.2
1° Lightband		-30	-15	2.8 (-1)	17.8		90	75	28.1 (30)	46.9
2° #1-1 Lightband		-30	-15	1.9 (1.7)	16.9		90	75	24.4 (30)	50.6
2° #1-2 Lightband		-30	-15	1.6 (1.9)	16.6		90	75	24.6 (30)	50.4
LV Lightband		-30	-15	-0.1 (6.9)	14.9		90	75	N/A	-

Unacceptable Margin
Acceptable margin

The first column states the raw operating temperature limits of each avionics box; usually given by the manufacturer. To satisfy the guidelines of the General Environmental Verification Specification (GEVS), a 15°C margin was added to the raw operating limit to create the design limit, 10°C for qualification testing and 5°C for modeling uncertainty. It is shown from the table that there is significant margin on the design limit.

The limiting component on the worst case hot scenario is the LCT2, where there is 18.3°C margin to the operating limit, and 3.3°C to the design limit. This is not surprising due to the fact the LCT2 produces the most amount of heat, estimated at 45W and shows the need for the LCT2 to be a radiator. The limiting component on the worst case cold scenario is the LCTE, where there is 23.8°C margin to the operating limit, and 8.8°C to the design limit. This is due to the fact the LCTE only produces about 4.8W of heat and is placed on the radiator doubler. There is no operating temperature limit for the battery charge and monitor box because it is not used during the flight. The battery charge and monitor box are only used to charge the MPE batteries and the attached payloads prior to payload encapsulation on the launch pad.

4.3.1 Worst Case Hot Predictions

Figure 6 visually shows the temperature gradients on the -Z avionics flange.

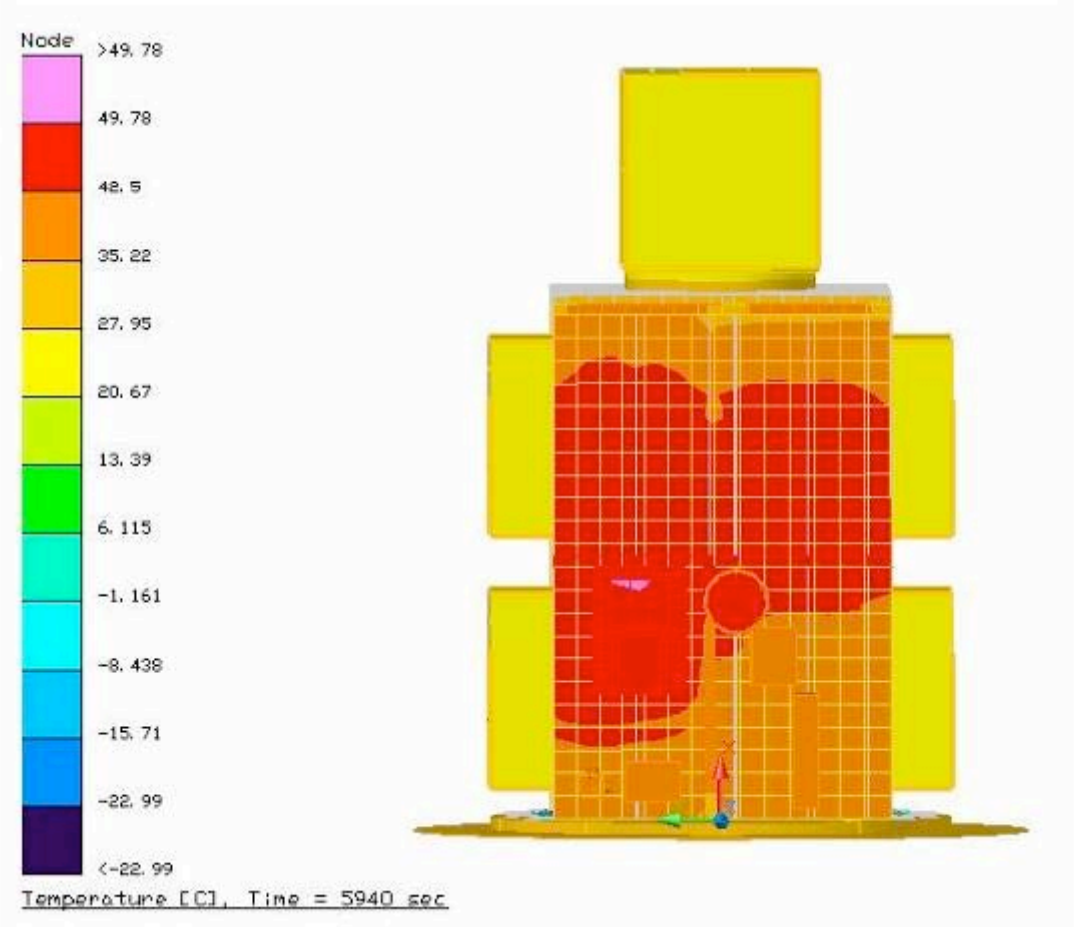

Figure 6 - -Z Avionics Worst Case Hot

The temperature gradients on the –Z avionics flange shows the hottest points are the LCT radiator. It also shows that the LCT2 and LCTE are adequately coupled to the radiator doubler, since there are no major temperature gradients within the radiator system. The antenna, covered in 10 mil silver Teflon tape, also heats up to a higher temperature than the rest of the system. The battery charge and monitor box, the MPE battery, the rate sensors, and the telemetry box also show that they are well coupled to the flange cover and are at the average sink temperature.

The Figure 7 shows the temperatures of the –Z avionics flange as a function of time throughout the flight.

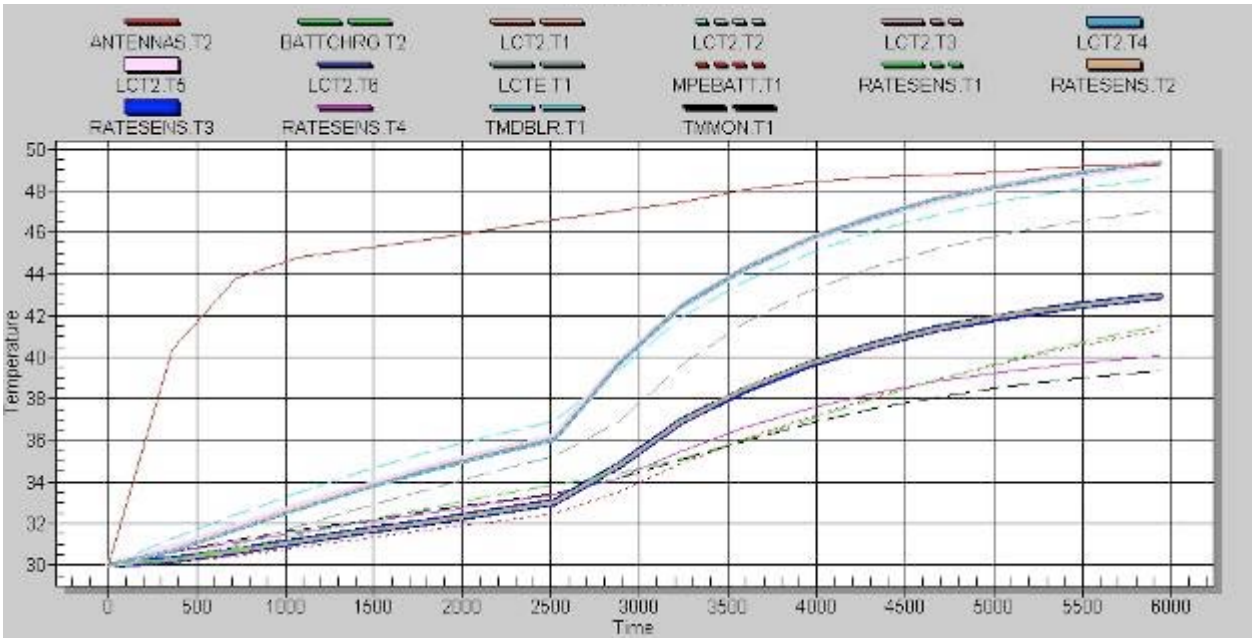

Figure 7 - -Z Avionics Temperature Graph

The antenna heats up fairly rapidly compared to the rest of MPE, which is expected due to the antenna's exposure to the external environment and its relatively low mass and poor conduction through the FR4 ground plane. The LCT2 and LCTE heat up faster than the rest of the avionics as the effective radiator is exposed directly to the solar flux. At 2700 seconds, the avionics begin to heat up more rapidly as the MPE receives the deployment signal from the launch vehicle.

Figure 8 shows the temperature gradients on the +Z avionics flange.

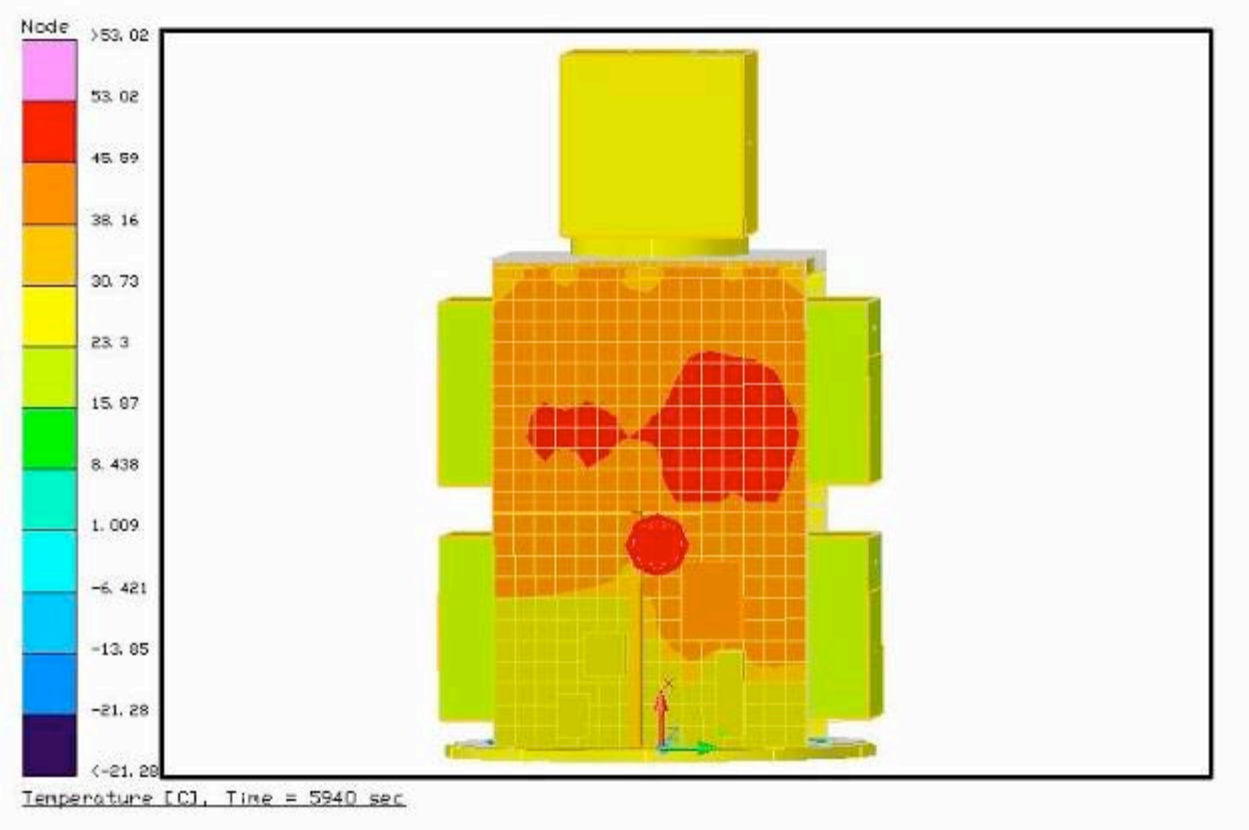

Figure 8 - +Z Avionics Worst Case Hot

The temperature gradients on the +Z avionics flange predict the hottest temperatures on the upper flange. Figure 8 is slightly deceiving, as the temperature gradients are only on the order of a few °C on the upper flange. The antenna covered in 10 mil silver Teflon tape also heats up higher than the rest of the system. The Power Out Box, the initiator battery, the timer box, and the enable relay box also show that they are well coupled to the flange cover and are at the average sink temperature.

Figure 9 shows the temperatures of the +Z avionics flange as a function of time throughout the flight.

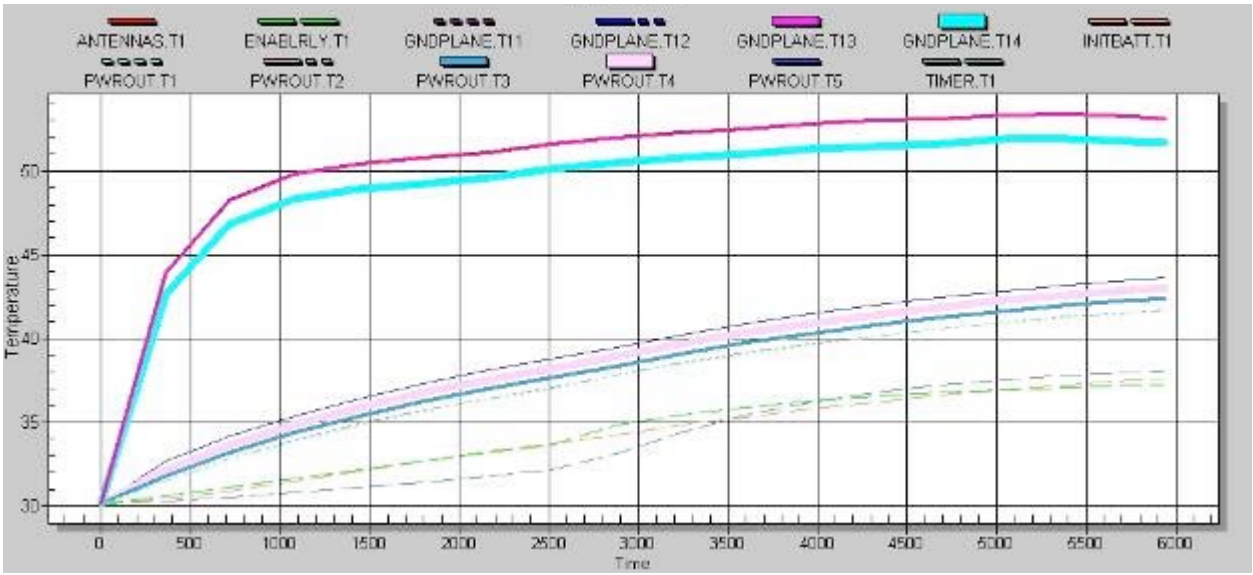

Figure 9 - +Z Avionics Temperature Graph

The antenna heats up rapidly compared to the rest of MPE, which is consistent with the –Z avionics flange in a different simulation run. The Power Out Box heats up faster than the rest of the avionics on this flange due to the added power dissipation and conduction from the localized heating in the upper flange to the lower flange. The deployment signal from the launch vehicle causes the avionics to heat up more quickly. The increase in temperature is not as pronounced in the –Z avionics flange, due to the lower consumption of power on the –Z avionics flange. All of these graphs show that the use of MLI blankets help keep the avionics close to its initial launch temperature throughout the mission. Even in the worst case hot environment of the avionics seeing direct solar flux, the MLI blankets perform very well in minimizing the heat absorbed by MPE. It is crucial to keep MPE hot biased, as there is no heater power available if the avionics drop in temperature towards their lower operational limit.

4.3.2 Worst Case Cold Predictions

Figure 10 shows the temperature gradients on the -Z avionics flange for the cold case.

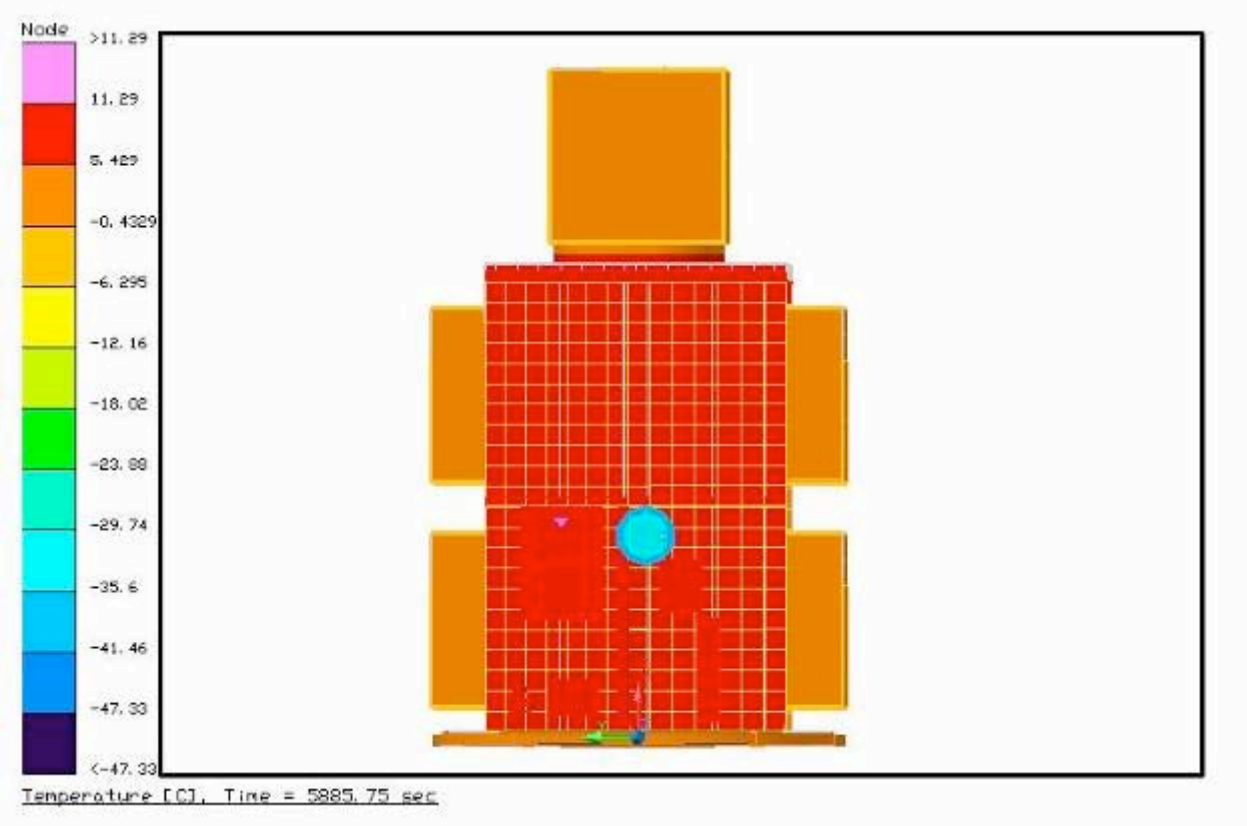

Figure 10 - -Z Worst Case Cold

The temperature gradients on the –Z avionics flange shows the coldest points are on the antenna assembly. The antenna covered in 10 mil silver Teflon tape cools down very rapidly as it sees primarily deep space. The average temperature of MPE and the avionics are approximately 8°C, with the LCT2 slightly higher around 11°C.

Figure 11 below shows the temperatures of the –Z avionics flange as a function of time throughout the flight.

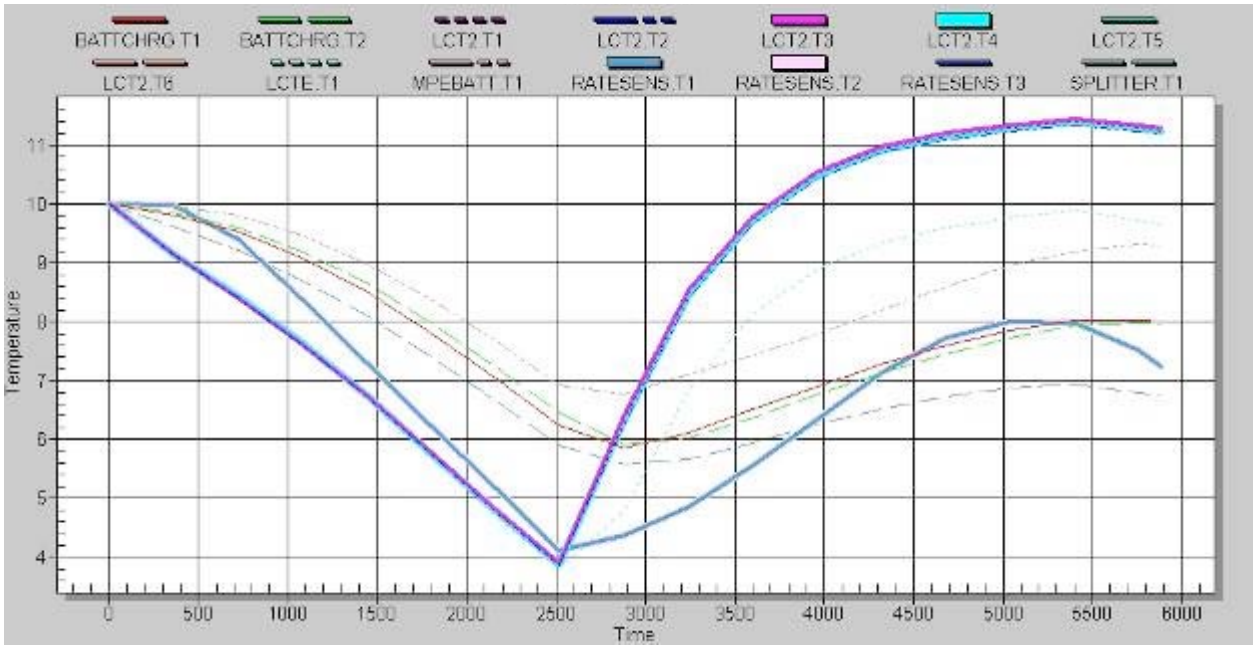

Figure 11 - -Z Avionics Temperature Graph

The LCT2 and LCTE cool down at a faster rate than the avionics under the MLI blankets during the 45 minute inactive coast. At 2700 seconds, the avionics begin to heat up as the MPE receives the deployment signal from the launch vehicle. The LCT2 increases in temperature approximately 7.5°C at the end of the 54 minute active portion and the LCTE increase in temperature approximately 3.5°C. All of the temperatures follow the anticipated trends seen in orbit.

Figure 12 visually shows the temperature gradients on the +Z avionics flange during the cold case.

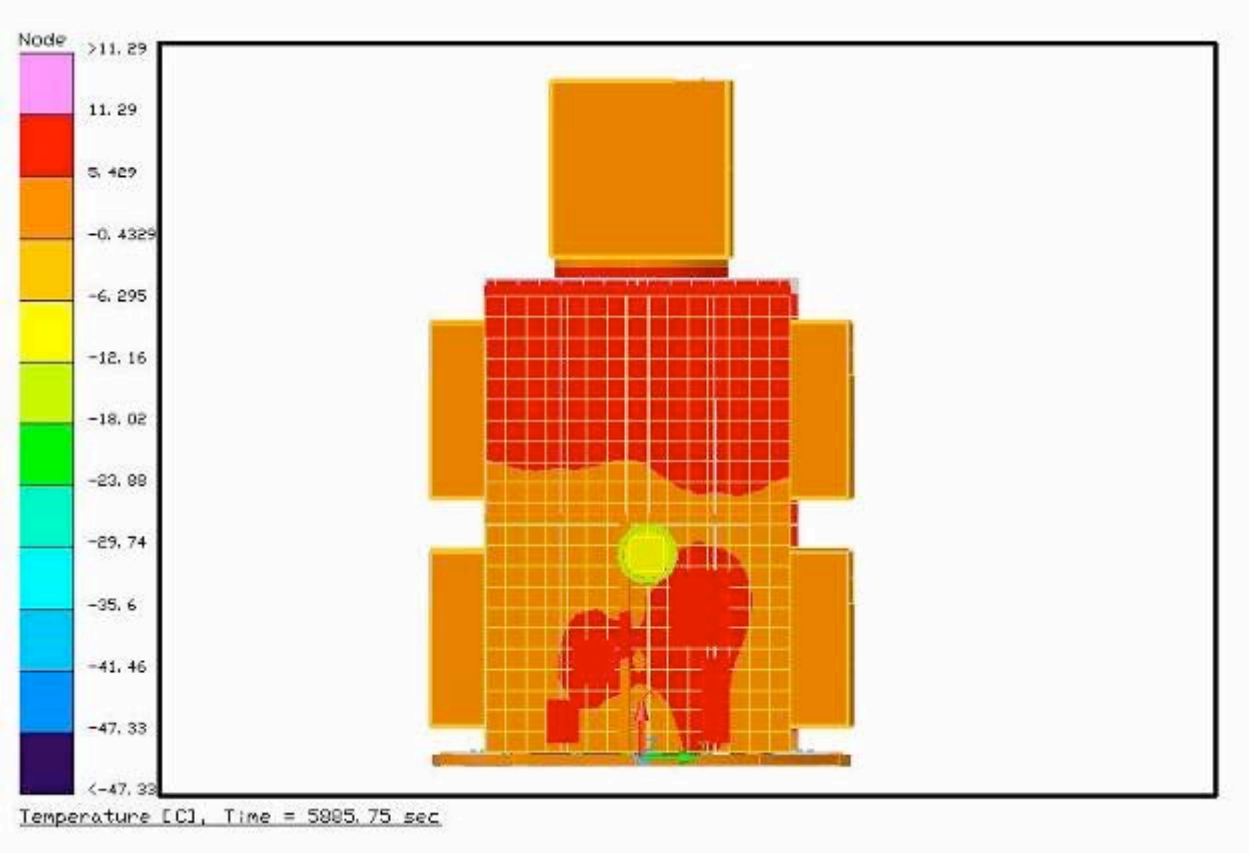

Figure 12 - +Z Avionics Worst Case Cold

The temperature gradients on the +Z avionics flange shows the coldest points are on the antenna assembly as well. The antenna covered in 10 mil silver Teflon tape cools down because of the harsh environment it experiences in deep space. The average temperature of MPE and the avionics are approximately 7°C at the end of the flight. There is some localized heating around the avionics boxes, but the overall gradients on the flange remain within 4°C.

Figure 13 shows the temperatures of the +Z avionics flange as a function of time throughout the flight.

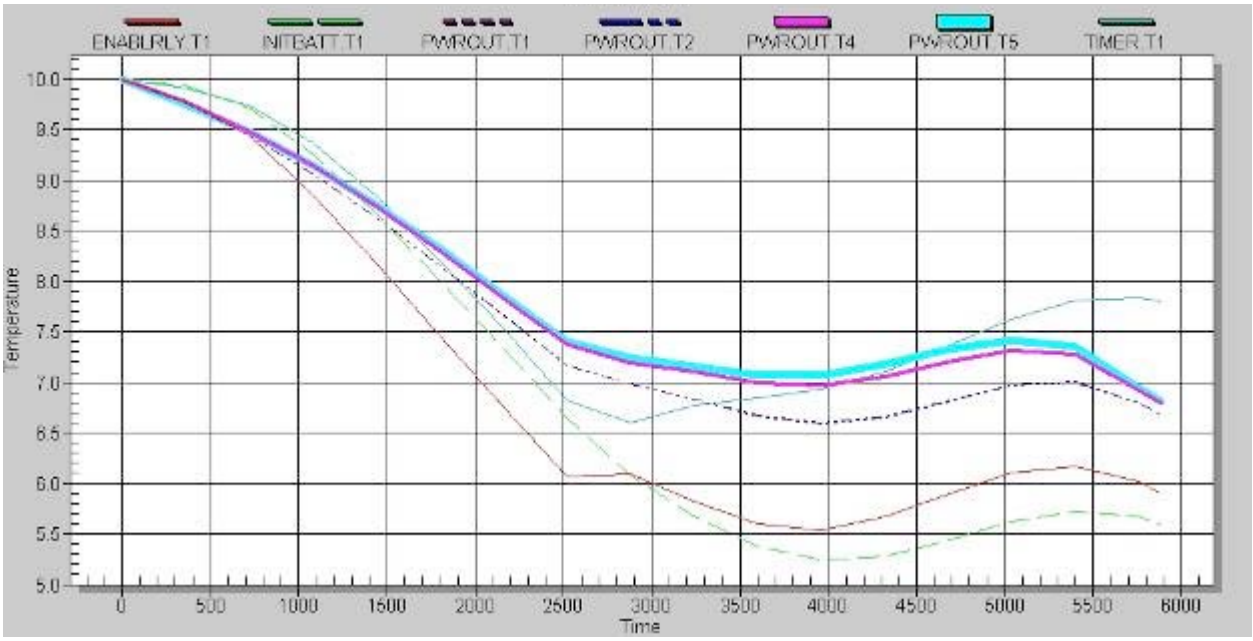

Figure 13 - +Z Avionics Temperature Graph

The avionics and MPE structure start at 10°C and begin to cool down as the MLI-covered flange sees primarily deep space for the 45 minute inactive coast. When MPE receives the deployment signal from the launch vehicle, the avionics temperatures begin to increase slightly. The temperature increase is not as pronounced as the –Z avionics flange because the majority of the power dissipation occurs in the telemetry system and the LCT2. All of these graphs show that the use of MLI blankets help keep the avionics close to its initial launch temperature throughout the mission. Even in the worst case cold environment where the avionics see deep space, the MLI blankets perform very well in minimizing the heat loss of MPE.

5. SYSTEM THERMAL VACUUM TEST

5.1 TEST BOUNDARY CONDITIONS

Since the MPE temperature control was conducted via heaters directly mounted to MPE, the control points were in locations near the avionics and the interface between the upper and lower flanges. The exception was the radiative heater panel placed in front of the LCT radiator to control the heat loss from the radiator. MPE structure temperatures were derived from model predictions and margin placed on the MPE average sink temperatures. For the hot thermal balance, MPE was maintained at 30°C, which is 15°C below the hot thermal cycle temperatures. For the cold thermal balance, MPE was maintained at 0°C, which is 11°C above the cold thermal cycle temperatures. For the thermal cycle temperature extremes, the MPE structure temperatures were chosen to stress the avionics as close to their operating limits without exceeding them. The set points of the thermal cycle temperatures could also be changed based upon the information provided during the hot and cold balances.

All temperature controllers operated nominally and followed their predicted temperature profile. The –Z avionics left interface increases in temperature from the baseline at all the operational plateaus due to the relatively close distance to the LCT radiator. The LCT temperature controller also transitions in temperature faster than the other interface points due to its relatively low mass and its highly emissive properties.

5.2 TEST OVERVIEW

The MPE thermal vacuum test was performed in the NASA thermal vacuum chamber in WFF building F-7 on September 12th 2007. Four thermal vacuum cycles with extended

hot and cold dwells on the first cycle for thermal balance were performed. Figure 14 shows MPE at the entrance of the chamber as final closeouts to the flight MLI blankets are being made.

Figure 14 - MPE Preparing to Enter the Thermal Vacuum Chamber

For purposes of model correlation, the MPE was in a "2-Stack" configuration. That is, the MPE consisted of two I-beam-like segments and one top plate with its cover plate. Three Planetary Systems Corporation Mk. II 15" Motorized Lightband (PSC Mk. II MLB) separation systems were present during the test, one for the primary and two in the secondary slots on the same side. Separation system mass mockups were used for the other two secondary slots. No payloads (or payload mock-ups/dummy payloads) were present during this test. All flight MLI blankets and tape coating schemes were present during the test. There was also MLI blankets covering the PSC Mk. II MLB during the test, but the blankets will not be present in the flight configuration. Flexible Kapton heaters were placed on the upper flange cover and on the launch vehicle adapter ring to

control the MPE structure temperature along with a radiative heater panel in front of the LCT Doubler to control heat loss. These heaters will not be present in the flight configuration.

All of the ground support equipment for the test operated nominally throughout the duration of the test, and the data acquisition system provided adequate data to perform test analysis. There were several correctable anomalies encountered during the pump down of the chamber to a high vacuum and also stabilizing the cryogenic shroud at -100°C. After adjusting the heater and LN2 settings for the shroud panels, all 12 panels were able to maintain and hold -100°C for the entire duration of the test. A detailed account of the status of the ground support equipment is available in the appendices.

All objectives of the test were satisfied and the test was declared a complete success. The MPE demonstrated that it was able to operate well beyond the worst case predicted temperature environments. MPE temperatures compared well to the model predictions, which confirmed the accuracy of the thermal model and the interfaces between the avionics and the structure.

5.3 TEST TIMELINE

The test was performed in one session from September 12th, 2007 through September 18th, 2007. The two thermal balance tests, the four thermal cycles, and all limited performance tests were performed. No uncorrectable electronic functional anomalies were encountered during the test.

9/12/07

- (0112 EST) The chamber is closed and the start of data logging occurs.

- (0320 EST) The chamber began the pump down to high vacuum.
- (2120 EST) Avionics were turned on for the start of the hot balance (operating on EGSE power).

9/13/07

- (0910 EST) Hot balance was declared.
- (0928 EST) Transition to the first hot soak occurs.
- (1224 EST) MPE has reached its hot set point and a 1 hour long LPT performed (operating on MPE battery power).
- (1335 EST) Hot restart of MPE occurred and transition to cold balance.
- (2216 EST) Cold balance has started and avionics were turned on (operating on EGSE power).

9/14/07

- (0615 EST) Cold balance was declared.
- (0722 EST) Transition to the first cold soak occurs.
- (0935 EST) Cold restart of MPE occurred and the cold soak starts (operating on EGSE power).
- (1052 EST) Conclusion of the first cold soak and transition to second hot soak.
- (2346 EST) Hot soak #2 is reached and avionics turned on for 1 hour (operating on EGSE power).

9/15/07

- (1000 EST) Cold soak #2 is reached and the avionics turned on for 1 hour (operating on half EGSE power and half MPE battery power).
- (1110 EST) Cold soak #2 concludes and transition to hot soak #3 begins.
- (1826 EST) Hot soak #3 is reached and the avionics turned on for 1 hour (operating on EGSE power).
- (1920 EST) Hot soak #3 concludes and transition to cold soak #3 begins.

9/16/07

- (0630 EST) Cold soak #3 is reached and the avionics turned on for 1 hour (operating on EGSE power).
- (0720 EST) Cold soak #3 concludes and transition to hot soak #4 begins.
- (1638 EST) Hot soak #4 is reached and the avionics turned on for 1 hour (operating on EGSE power).
- (1732 EST) Hot soak #4 concludes and transition to cold soak #4 begins.

9/17/07

- (0735 EST) Cold soak #4 is reached and the avionics turned on for 1 hour on battery power.
- (0825 EST) MPE batteries are completely drained and the LPT must be stopped. The minimum 54 minute flight time was not achieved.
- (1230 EST) MPE is brought back to room temperature and battery charging ass performed. It was found out that batteries were only being charged to 80%, and now with the fully topped off batteries, the 54 minute minimum flight time should

be satisfied.

- (2125 EST) MPE performs cold soak #5 to satisfy requirement.
- (2235 EST) Successful completion of cold soak #5 on battery power and MPE ramped back up to room temperature.

9/18/07

- (0230 EST) Ambient conditions are reached.

5.4 THERMAL BALANCE PREDICTIONS

Because MPE is a short-duration mission, its design requires it to survive for as little as 99 minutes (dual-impulse insertion to LEO plus a timer lifetime of 54 minutes). Since no power is available for heaters (and would be inaccessible and thus useless during a 45 minute inactive coast for the 2-impulse case), the MPE's design is transient in nature. Thus, orbit-average effective sink temperatures are not appropriate, as temperatures are still moving at the end of a nominal mission profile and not cycling about an "orbit average" temperature. Therefore, the main goal of the thermal balance is to correlate the thermal model and not to determine "orbit average" temperatures.

Table 4 compares the thermal balance predictions from the Thermal Desktop model and the actual thermal balance temperatures from the test. The major assumptions in the thermal model are the power generation of each avionics box and the interface conductance between the avionics boxes and the MPE structure. The uncertainties in the power generation numbers come from the lack of actual measurement during the comprehensive performance test. Only certain avionics boxes actually measure the

voltage drop across the box and measure inline current readings. The heat generation of the LCT2 was calculated by subtracting the RF power out from the actual consumption of the box, which totaled 45W of waste heat. Grafoil interface material was used for all boxes as the avionics interface to the MPE structure. The advertised thermal conductivity of the Grafoil is 12 $W*m^{-1}*K^{-1}$, however past experiences have placed the actual thermal conductivity at only 25% of the advertised thermal conductivity. As a conservative approach, only 3 $W*m^{-1}*K^{-1}$ was used. The temperatures from the test are sampled at the top of every avionics box, with the normal facing in the +Z/-Z avionics directions. This assumes that the interior temperatures are well coupled to the exterior of the box.

The LCT2 was the most critical component in the hot balance due to its heat generation. There is a 5.7°C difference between the predicted and actual balance temperatures, where the actual value was lower than predicted. Even though there is a 5.7°C difference, it is beneficial to know that the model is predicting a worse case than what actually happens. The difference could be attributed to the fact that the LCT2 doesn't not necessarily produce the full 45W of waste heat and that the Grafoil interface is more efficient than 25% of its advertised value. The observation that the Grafoil is more efficient than 25% is apparent in all of the temperatures, as the actual test temperatures are all below the thermal balance predicted temperatures. The MPE battery can also be assumed not to produce 15.5W of heat and is much closer to the Initiator battery temperature and heat generation. The thermal interface conductance values along with power numbers will be updated in the thermal model to better correlate it with the actual results.

The LCTE was the most critical component in the cold balance due to its lower heat generation and being an effective radiator. There is a 3.75°C difference between the

predicted and actual balance temperatures, where the actual value was lower than what was predicted. The difference could be attributed to the fact that the LCTE does not produce the full 4.8W of waste heat and that the Grafoil interface is more efficient than 25% of its advertised value. All of the predicted temperatures are within acceptable limits; the data correlates well. The Power Out Box is slightly higher than the predicted temperature by about 7.5°C. This difference could be attributed to the multiple layers of the Power Out Box, where all layers are not isothermal and the 5V and 12V regulators on each board would provide localized heating. The thermal interface conductance values along with power numbers are updated in the thermal model to better correlate it with the actual results.

Table 4 - Thermal Balance Comparisons

Thermal Balance Temperature Comparison									
		Cold				Hot			
MPE Avionics		Power Dissipated (°C)	Raw Limit (°C)	T/B Prediction (°C)	T/B Actual Test Data (°C)	Power Dissipated (°C)	Raw Limit (°C)	T/B Prediction (°C)	T/B Actual Test Data (°C)
Timer		0.84	-20	3.11	0.5	0.84	60	36.1	29.75
LCT2 Transmitter		45	-24	15	13.5	45	65	47.2	41.5
LCTE		4.8	-20	13.5	9.75	4.8	75	45.7	37.75
Telemetry Monitor		0.51	-20	1.5	4.0	0.51	85	41.9	33.25
MPE Battery		0.0	-20	0.2	0.5	15.5	60	44.1	30.75
Initiator Battery		0.65	-20	0.2	1.5	0.65	60	33.2	31.25
Rate Sensors		1.2	-40	10	10.0	1.2	80	42.3	37.5
Battery Charge Box		0	-	0.1	3.0	0	-	42.5	31.6
Battery Monitor Box		0	-	0.1	3.0	0	-	42.5	31.6
Power Output Box		0	-30	0.06	7.5	0	80	33.1	36.0
Relay Box		4.61	-65	0.8	1.25	4.61	125	33.8	31.75
Antennas		0	-100	-5.8	-4.0	0	121	28.4	21.75

5.5 HOT THERMAL BALANCE

Figure 15 and Figure 16 show temperatures of the +Z/-Z avionics for the 8 hour hot thermal balance. The minimum duration for the hot thermal balance was 6 hours, but at the conclusion of the 6 hours, there were noticeable oscillations in the temperature of the avionics boxes. The oscillations appeared to have the same period of 2 hours for each avionics box and remained constant through the duration of the hot balance. The amplitudes started as high as 4°C in the telemetry box and slowly started to decay to approximately 1°C in 3 full periods. If these oscillations were caused by cycling power in the MPE avionics, the amplitude of the oscillations would not necessarily decrease at this rate, but the amplitude would remain fairly constant over an 8 hour time period. A likely cause of the oscillations could be the Harrel heater rack and the dead band of the Harrel controller. After observing the simple control method of the Harrel heater rack, it was noted that the dead band of the Harrel heater rack could range from 1°C up to as

much as 4°C. This could explain the oscillations and the decrease in amplitude as the Harrel heater rack settles out.

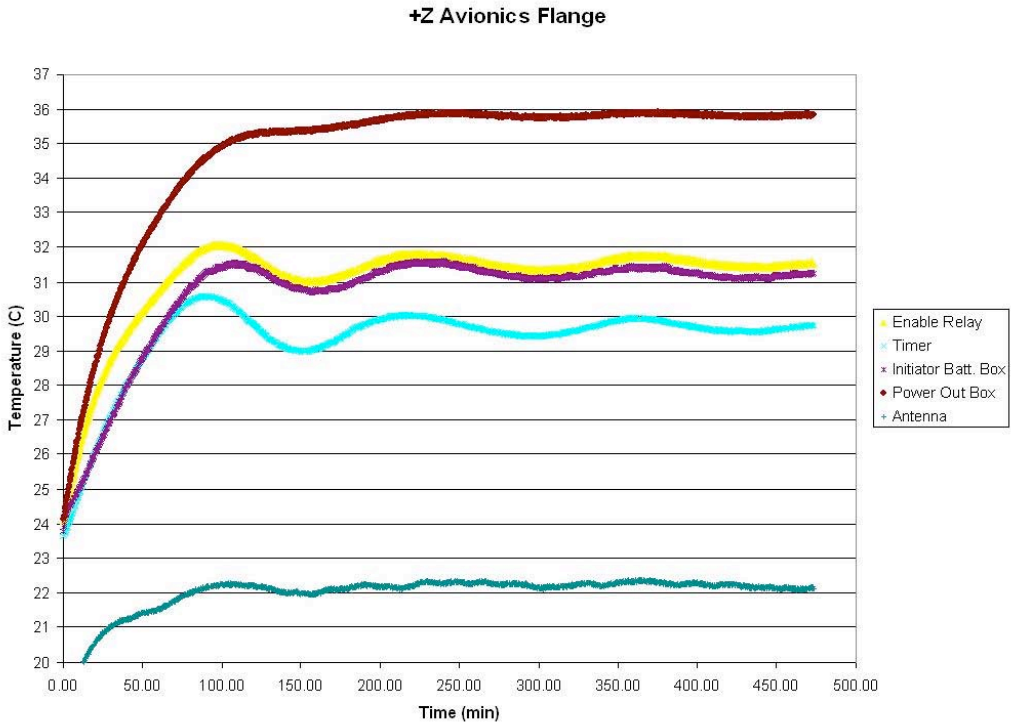

Figure 15 - +Z Avionics Hot Balance Temperature Graph

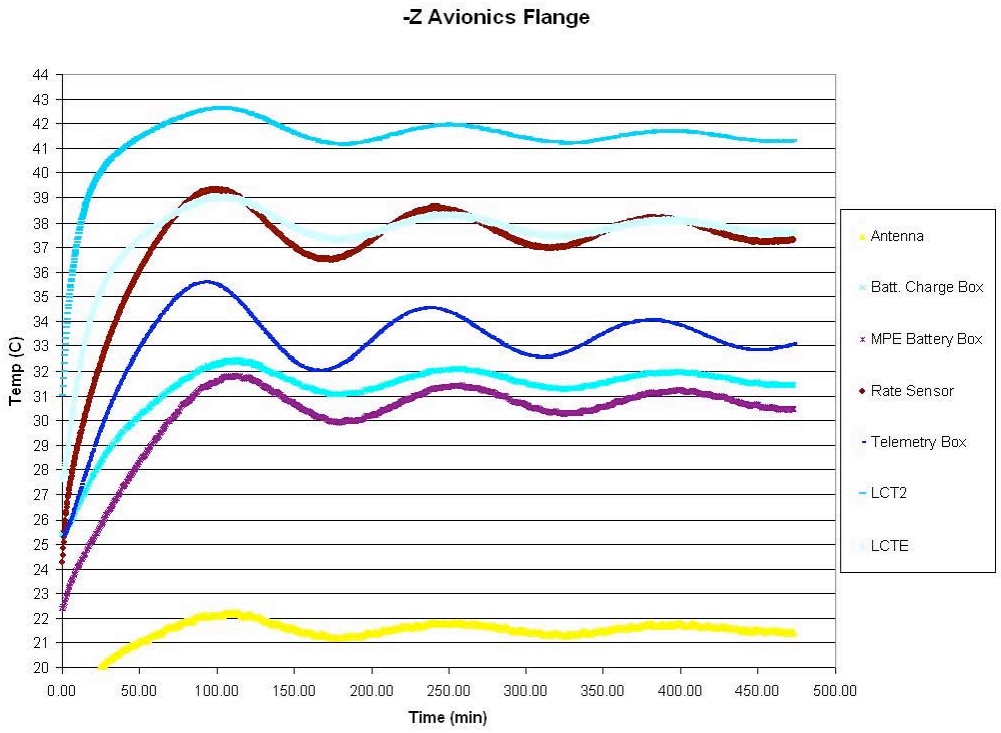

Figure 16 - -Z Avionics Hot Balance Temperature Graph

5.5.1 Hot Thermal Balance Criteria and Determination

The minimum temperature stabilization criteria for the thermal hot balance is no temperature measurement should exceed a 0.09°C/hr rate of change for at least six hours and exhibit a decreasing slope over this time frame. There was no simple way to determine this criteria, so the data was analyzed using Excel. Because of the oscillations the temperatures did not stabilize to 0.09°C/hr for any given point in time. A linear line fit of the data was used to approximate the converging slopes of the oscillation. Caution was taken to capture only full periods of the oscillations because any fraction thereof would negatively affect the line of best fit. Table 5 shows the temperature rates of the avionics after 8 hours. Appendix A has individual plots of each avionics box's temperature with the line of best fit. The slope should be multiplied by 60 to compare the

°C/hr rate, as the slope is in °C/min rate.

Table 5 - Hot Balance Temperature Rates of Change

+Z Flange		-Z Flange	
Thermocouple	ΔT/Δt (°C/hr)	Thermocouple	ΔT/Δt (°C/hr)
Antenna	0.012	Antenna	-0.024
Enable Relay Box	0.03	Battery Charge Box	-0.012
Initiator Battery Box	0.042	LCT2	-0.054
Power Out Box	0.06	LCTE	-0.0018
Timer Box	-0.018	MPE Battery Box	-0.006
		Rate Sensors	-0.066
		Telemetry Box	-0.03

All of the hot balance temperature rates of change are within the 0.09°C/hr criteria. The 8 hour soak allowed the oscillations to dampen sufficiently to satisfy the requirement. The highest rate of change occurred with the rate sensors. These rate sensors have a low thermal mass compared to the rest of the avionics boxes and are susceptible to greater fluctuations in temperature. The LCT2 also has a high temperature rate of change, which would be due to the higher heat generation of 45W and being exposed to the LCT radiator panel.

5.6 COLD THERMAL BALANCE

Figure 17 andFigure 18 of the +Z/-Z avionics show temperatures for the 8 hour cold thermal balance. The minimum duration for the cold thermal balance was also 6 hours, but oscillations in the temperature of the avionics boxes were present. The oscillations appeared to be slightly different than the hot balance with a longer, more erratic period. The amplitudes started at 2°C in the timer box and decay to less than 1°C in 3 full periods. These oscillations were not caused by cycling power in the MPE avionics, as apparent in the –Z avionics, where the oscillations are not pronounced as much in the +Z

avionics flange in the cold balance and the –Z avionics flange in the hot balance . The Harrel heater rack may have caused these oscillations as well. The dead band range could explain the oscillations and the decrease in amplitude.

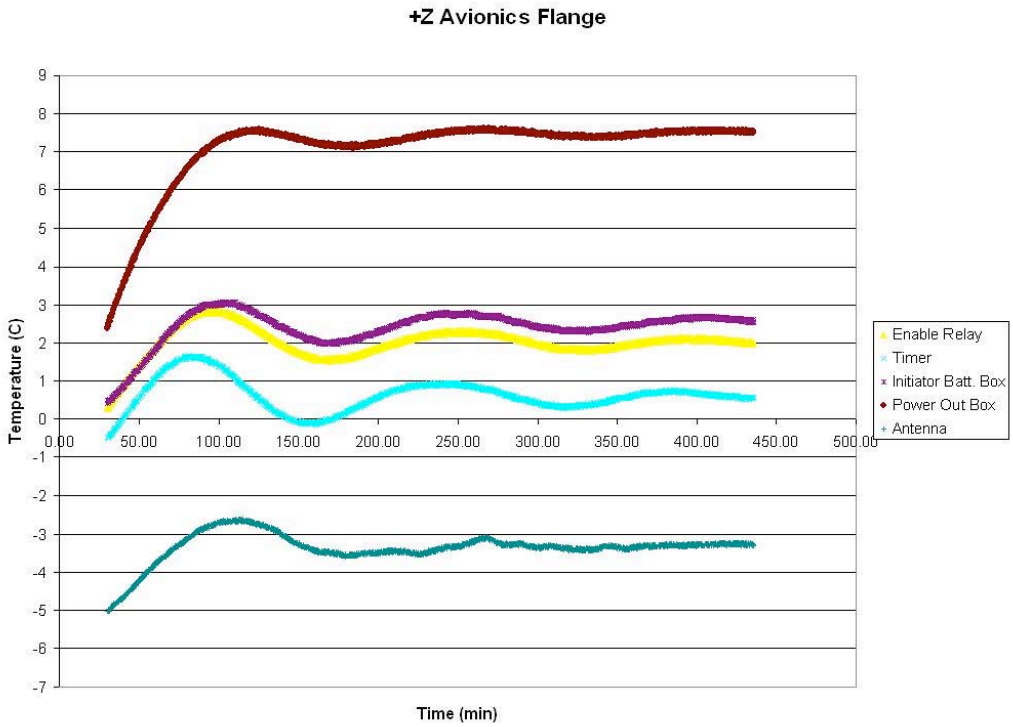

Figure 17 - +Z Cold Balance Temperature Graph

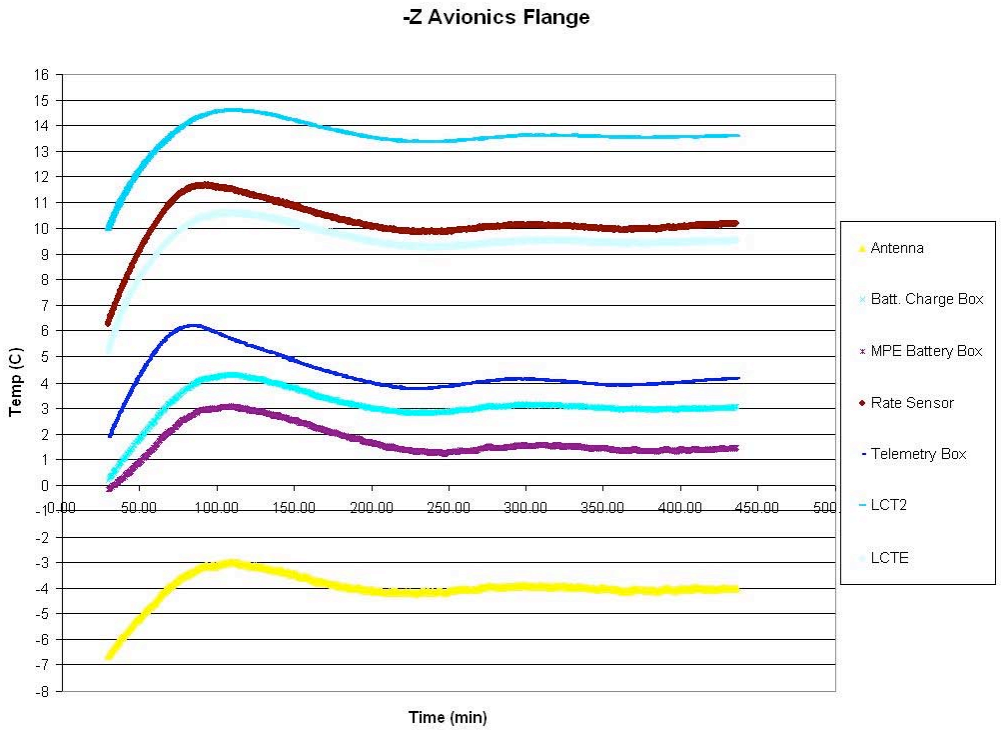

Figure 18 - -Z Cold Balance Temperature Graph

5.6.1 Cold Thermal Balance Criteria and Determination

The minimum temperature stabilization criteria for the thermal cold balance is no temperature measurement should exceed a 0.07°C/hr rate of change for at least six hours and exhibit a decreasing slope over this time frame. This temperature rate of change is consistent with a temperature rate of change less than 1% of the MPE total energy. Since the MPE has less total energy at 0°C than compared at 30°C, the temperature rate of change is also lower for the cold balance than for the hot balance. The oscillations in temperature required a curve fit since the temperatures did not stabilize to 0.07°C/hr for any given point in time. Only full periods of the oscillations were captured for accuracy. Table 6 shows the temperature rates of the avionics after 8 hours. Appendix B has individual temperature plots for each avionics box with the line of best fit. Please note

that the slope is in °C/min rate, while Table 6 is in °C/hr rate.

Table 6 - Cold Balance Temperature Rates of Change

+Z Flange		-Z Flange	
Thermocouple	ΔT/Δt (°C/hr)	Thermocouple	ΔT/Δt (°C/hr)
Antenna	0.042	Antenna	0.012
Enable Relay Box	0.012	Battery Charge Box	-0.012
Initiator Battery Box	0.042	LCT2	-0.012
Power Out Box	0.036	LCTE	0.03
Timer Box	-0.03	MPE Battery Box	-0.039
		Rate Sensors	-0.048
		Telemetry Box	-0.018

All of the cold balance temperature rates of change are within the 0.07°C/hr criteria. The 8 hour soak reduced the oscillations enough to satisfy the requirement. The highest rate of change was observed with the rate sensors, which is also consistent with the hot balance. These rate sensors have a low thermal mass compared to the rest of the avionics boxes and are susceptible to greater fluctuations in temperature.

5.7 QUALIFICATION THERMAL VACUUM CYCLE TESTING

The soak goal temperatures during thermal cycling were obtained from the thermal analysis of the MPE in the test chamber. The temperatures of the chamber and test heater settings for the TVAC temperature soaks were chosen to subject the components to 15°C beyond the worst mission operating scenarios, depending on their proximity to component operating temperature limits. The MPE average sink temperatures for the mission flight hot and cold operating scenarios were used, which were 30°C and 4°C respectively. The control thermocouples were placed at the flange interfaces and the launch vehicle adapter ring interface. The location of these control thermocouples also included the Harrel heater rack RTDs, which controlled the flexible Kapton heaters.

When all thermocouples were within 2°C of its goal, then the soak was considered to start. Figure 19 shows the control thermocouples.

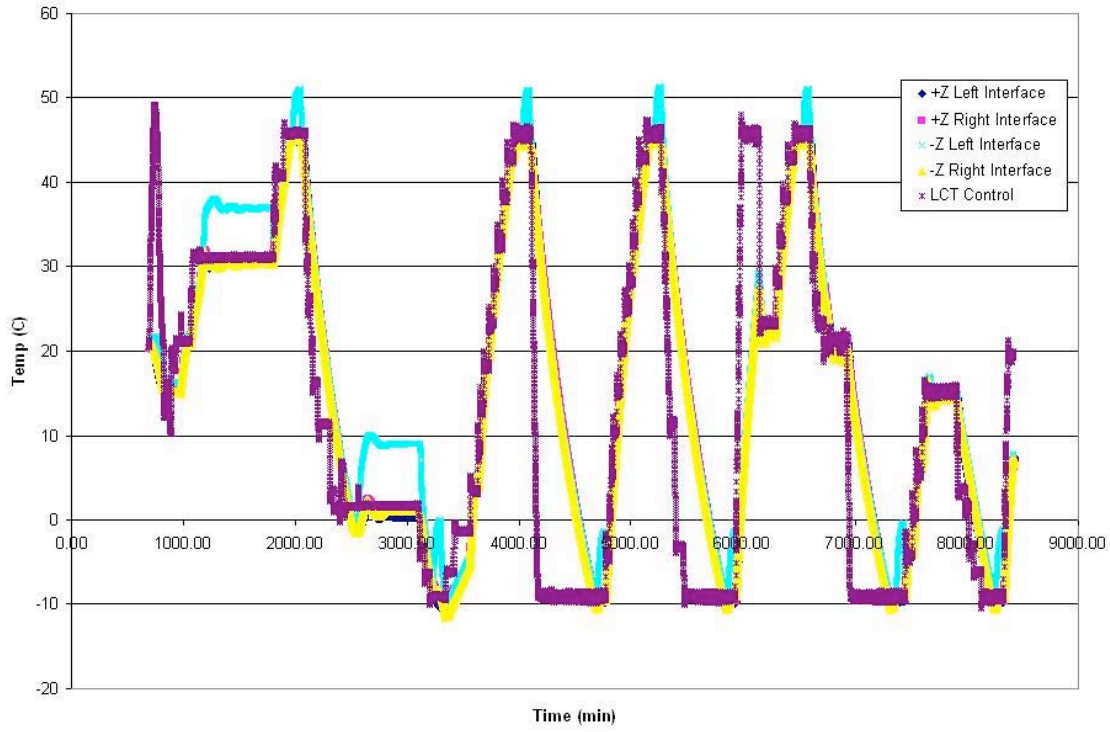

Figure 19 - MPE Control Theromocouple Temperatures

The visible –Z Right Interface line follows the baseline temperature profile, along with the +Z Left and Right Interface temperatures. The initial drop at the beginning of the test occurred when the chamber shroud panels were ramped to -100°C.As the heaters turn on, the temperature stabilizes again at approximately 20°C. During the fourth thermal cycle, the temperature steadies at 22°C during the ramp to hot cycle #4 and cold cycle #4 because of battery charging. The fifth cold cycle in the graph was due to insufficient charging of the batteries. During the fourth cold cycle, the avionics needed to be turned off at 50 minutes due to low battery power. This did not satisfy the minimum requirement of 54 minutes of active flight time. It was discovered that the batteries were

only being charged to 80% capacity not only during this test, but at all prior comprehensive and limited performance tests. With the batteries being fully charged, the fifth cold thermal cycle was able to satisfy the 54 minute minimum active flight time.

The visible –Z Left Interface line follows the baseline temperature profile during the ramps, but deviates at each temperature plateau. The location of the control thermocouple near the LCT radiator causes this behavior. When the LCT2 transmits and heats up, the heat is spread throughout the LCT doubler and migrates to the control thermocouple. This is positive confirmation, showing the heat generated by the LCT2 and LCTE is able to conduct adequately to the LCT doubler and then to the surrounding flange cover.

The LCT control thermocouple deviates significantly from the baseline temperature profile, as the LCT radiator is decoupled conductively from the MPE structure with G10 fiberglass standoffs. The LCT radiator is also low in thermal mass and has the advantage of changing temperatures very rapidly. This is desirable in the event that the LCT2 overheats and goes beyond its operating temperature limits and corrective action can be taken by dropping the temperature of the LCT radiator quickly.

5.7.1 Thermal Cycle General Test Results

According the Thermal Desktop model, the limiting component for the hot cycle was the LCT2. This was also confirmed in the thermal balance predictions and results. After analyzing the thermal balance data, the Thermal Test Director adjusted the upper temperature limits of the hot cycle. The LCT2 was operating approximately 5°C cooler than what was predicted. The Thermal Test Director had the opportunity to increase the hot cycle temperature to 50°C based on this information, but decided to remain with the

original 45°C prediction. The reason for this decision was to err on the side of caution for the first hot cycle, since the hot cycle temperature limit could always be increased on the subsequent cycles. During the first hot cycle, the LCT2 reached a temperature of 56°C, which followed the previous trend of the hot thermal balance. After discussions with the functional engineers, it was noted that the internal temperatures of the LCT2 were indeed reaching up to 62°C near the FPGA. Even though the manufacturer's operating temperature limits were based upon case temperatures, it was decided not to overstress the LCT2 in fear of exceeding the 65°C operating limit and damaging flight hardware. The 45°C hot cycle control temperature would remain the baseline throughout the test. It should be noted that even though the LCT2 was not stressed to within 5°C of its operating limit, it did reach within 9°C of its operating limit and exhibited +10°C margin above the maximum flight predicted environments.

According the Thermal Desktop model, the limiting components for the cold cycle were the LCTE, MPE and Initiator Batteries based upon their -20°C lower temperature operating limit. However the LCTE was a more critical component since its position on the LCT doubler would radiate more of its energy to space, while the MPE and Initiator batteries were shielded under the MLI blankets. This was also confirmed in the thermal balance predictions and results as well. After analyzing the data from the thermal balance, the Thermal Test Director chose to adjust the temperature limits of the cold cycle. It was observed that the LCTE was operating approximately 3.5°C cooler than what was predicted. The -11°C cold cycle control temperature would remain the baseline throughout the test. The LCTE was not stressed to within 5°C of its operating limit, but it did reach to within 9°C of its operating limit and exhibited +15°C margin below the cold

flight predicted environments.

During the thermal cycle testing, all avionics operated nominally throughout the entire duration and according to the functional engineers, there was no degradation in performance when comparing the pre- and post- comprehensive performance tests. A hot restart during the first hot cycle and a cold restart during the first cold cycle were also demonstrated. There was significant margin shown between the worst case predicted temperature environments and the thermal cycle limits.

5.8 COMPONENT SPECIFIC RESULTS

5.8.1 +/- Z Antennas

The cold raw operating temperature limit for the Seavey Engineering microstrip patch antennas is -100°C. After discussions with Seavey engineers, it was determined the -100°C limit came from qualification testing. Seavey is confident that the microstrip path antennas are able to operate at much lower temperatures as long as no mechanical strike impacts the antenna, since all the materials in the antenna are inert and contain no electronics. The main concern for the antennas was the hot case, so 10 mil silver Teflon was applied to the ground plane. However, during the cold case this would cause the antennas to become extremely cold when analyzed individually as a component. Given that the actual conductance to the MPE structure was unknown, caution needed to be taken during the test. The thermal model predicted a cold balance temperature of -5.8°C, and the actual cold balance temperature was -4.0°C. The thermal model predicted a cold cycle temperature of -21.4°C, and the actual cold cycle temperature was -16.2°C. This would suggest that the antennas were conductively coupled better to the MPE structure

than what the model predicted, and the silver Teflon did not negatively impact the temperature of the antennas. According to the thermal pass/fail criteria, there is a 65.2°C margin to the raw operating temperature limit.

The hot raw operating temperature limit for the Seavey Engineering microstrip patch antennas is 121°C. The thermal model predicted a hot balance temperature of 28.4°C, and the actual hot balance temperature was 21.8°C. The thermal model predicted a hot cycle temperature of 49.6°C, and the actual hot cycle temperature was 34.7°C. According to the thermal pass/fail criteria, there is a 74.6°C margin to the raw operating temperature limit.

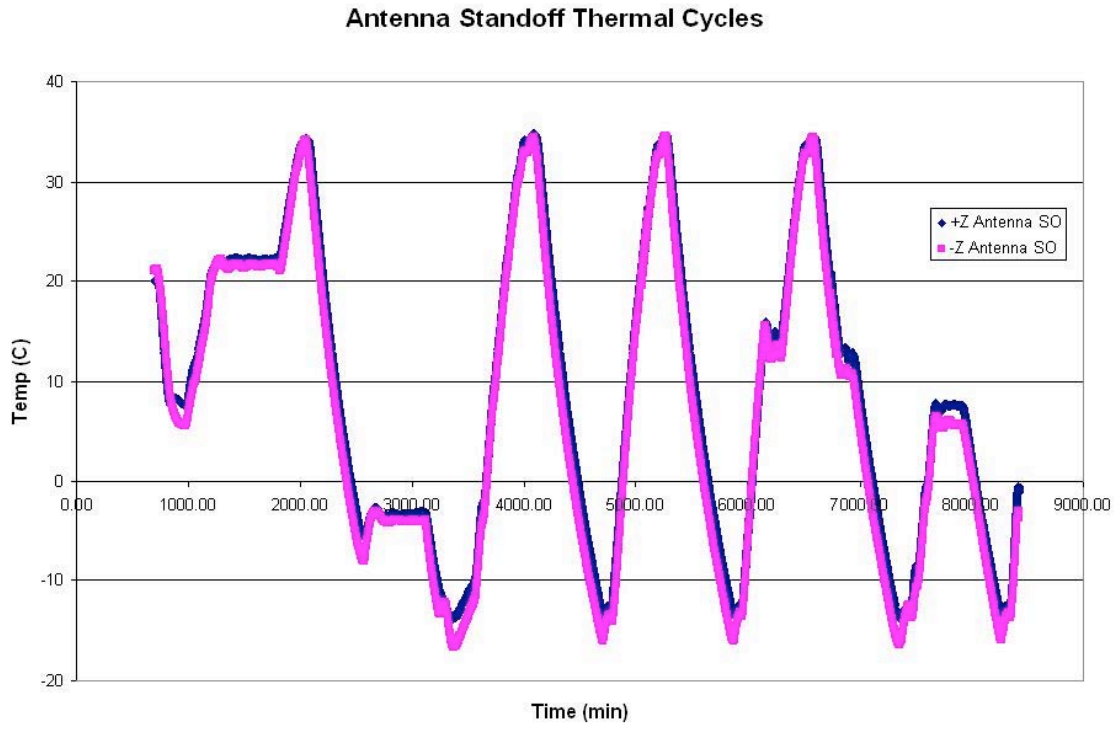

Figure 20 - Antenna Temperature Graph

5.8.2 Enable Relay Box

The cold raw operating temperature limit for the Enable Relay Box is -65°C. The

thermal model predicted a cold balance temperature of 0.8°C, and the actual cold balance temperature was 1.3°C. According to the thermal pass/fail criteria, there is 71°C of margin to the raw operating temperature limit.

The hot raw operating temperature limit for the Enable Relay Box is 125°C. The thermal model predicted a hot balance temperature of 33.8°C, and the actual hot balance temperature was 31.8°C. According to the thermal pass/fail criteria, there is 90°C of margin to the raw operating temperature limit.

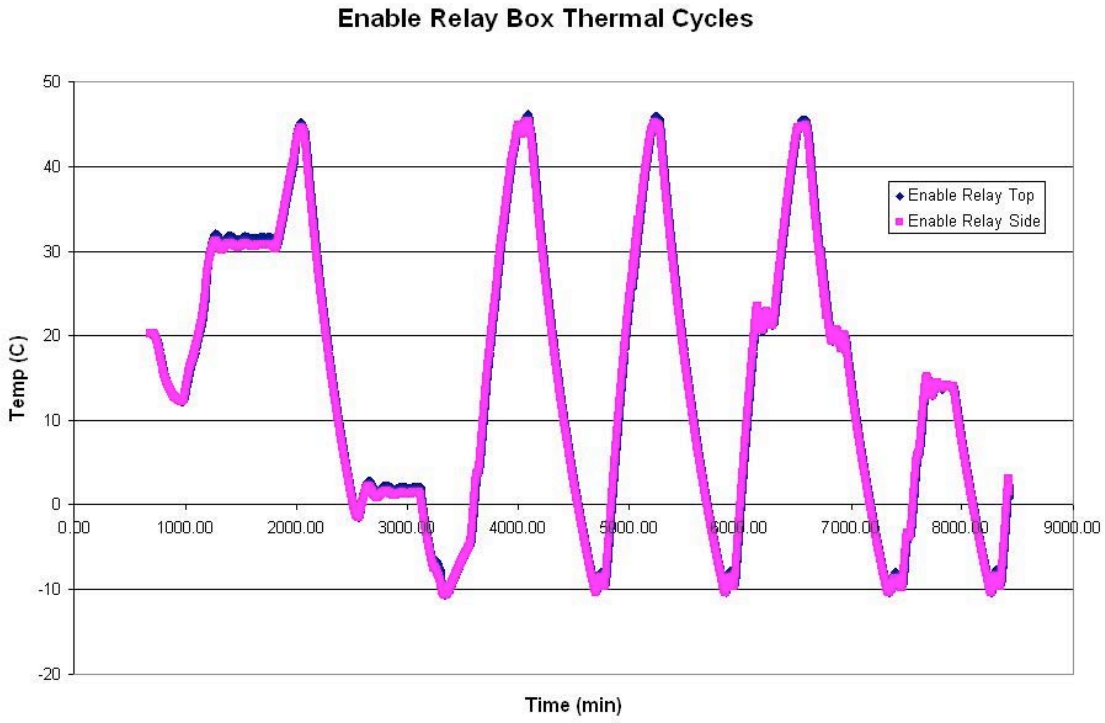

Figure 21 - Enable Relay Temperature Graph

5.8.3 Initiator Battery Box

The cold raw operating temperature limit for the Initiator Battery Box is -20°C. The thermal model predicted a cold balance temperature of 0.2°C, and the actual cold balance temperature was 1.5°C. According to the thermal pass/fail criteria, there is 26.5°C of

margin to the raw operating temperature limit.

The hot raw operating temperature limit for the Initiator Battery Box is 60°C. The thermal model predicted a hot balance temperature of 33.2°C, and the actual hot balance temperature was 31.3°C. According to the thermal pass/fail criteria, there is 23.4°C of margin to the raw operating temperature limit.

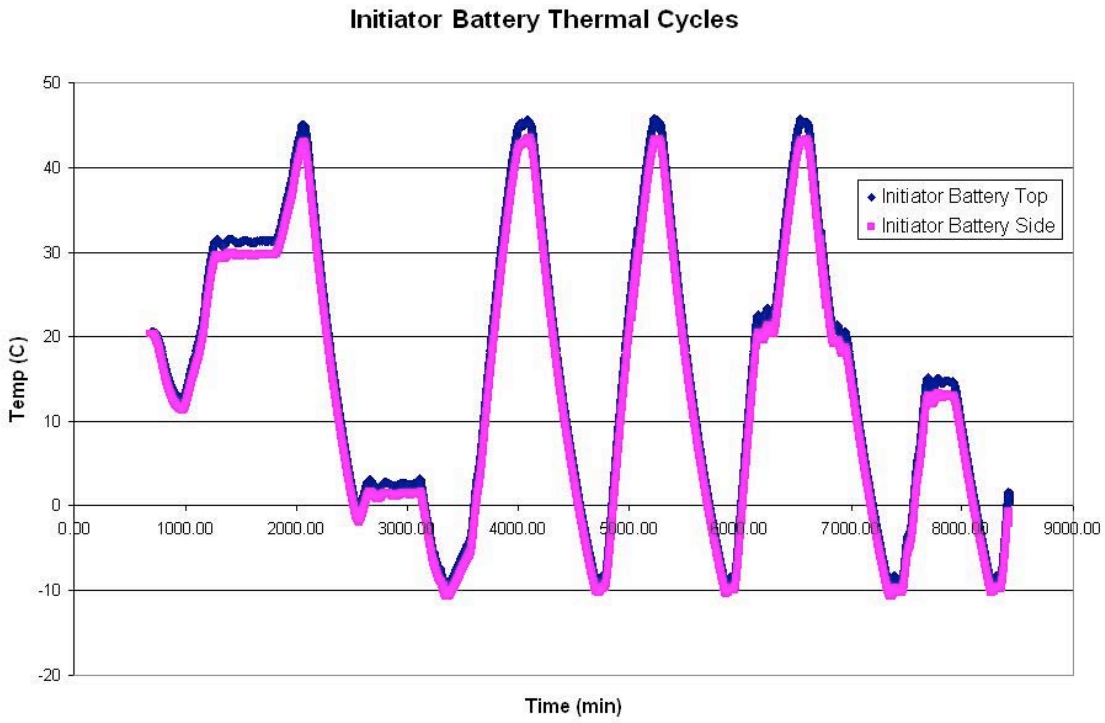

Figure 22 - Initiator Battery Temperature Graph

5.8.4 Power Out Box

The cold raw operating temperature limit for the Power Out Box is -30°C. The thermal model predicted a cold balance temperature of 0.1°C, and the actual cold balance temperature was 7.5°C. According to the thermal pass/fail criteria, there is 44.0°C of margin to the raw operating temperature limit.

The hot raw operating temperature limit for the Power Out Box is 80°C. The thermal model predicted a hot balance temperature of 33.1°C, and the actual hot balance temperature was 36.0°C. According to the thermal pass/fail criteria, there is 39.4°C of margin to the raw operating temperature limit.

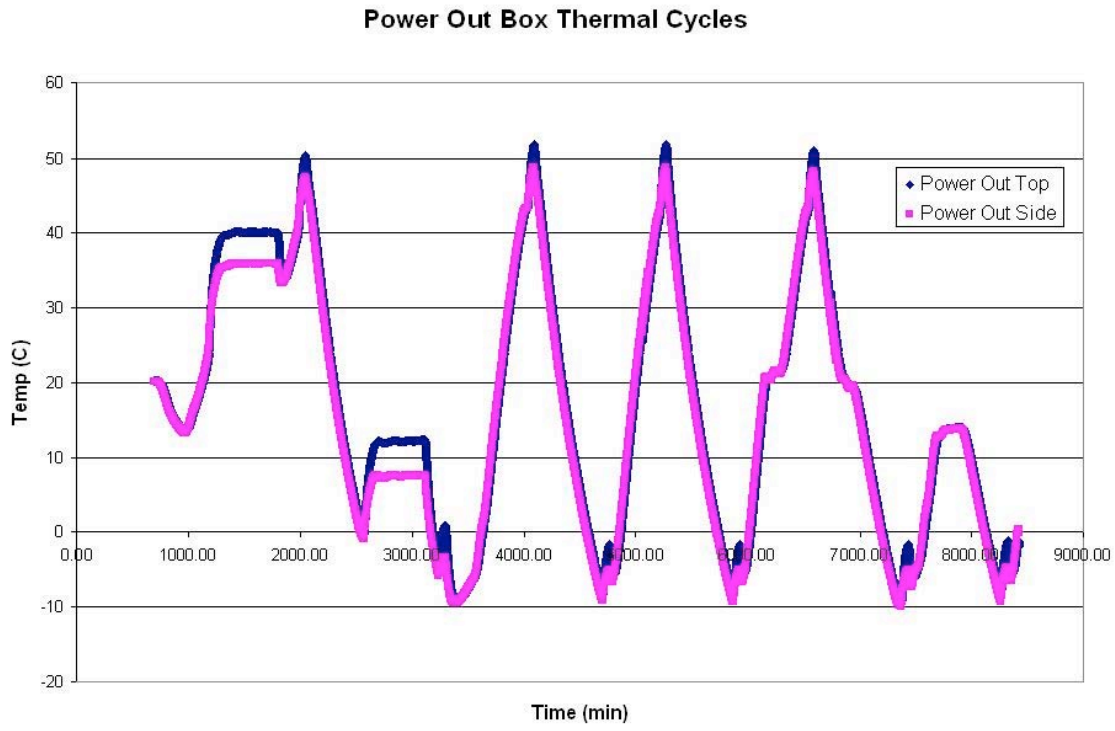

Figure 23 - Power Out Temperature Graph

5.8.5 Timer Box

The cold raw operating temperature limit for the Timer Box is -20°C. The thermal model predicted a cold balance temperature of 3.1°C, and the actual cold balance temperature was 0.5°C. According to the thermal pass/fail criteria, there is 24.0°C of margin to the raw operating temperature limit.

The hot raw operating temperature limit for the Timer Box is 60°C. The thermal model predicted a hot balance temperature of 36.1°C, and the actual hot balance temperature

was 29.8°C. According to the thermal pass/fail criteria, there is 28.4°C of margin to the raw operating temperature limit.

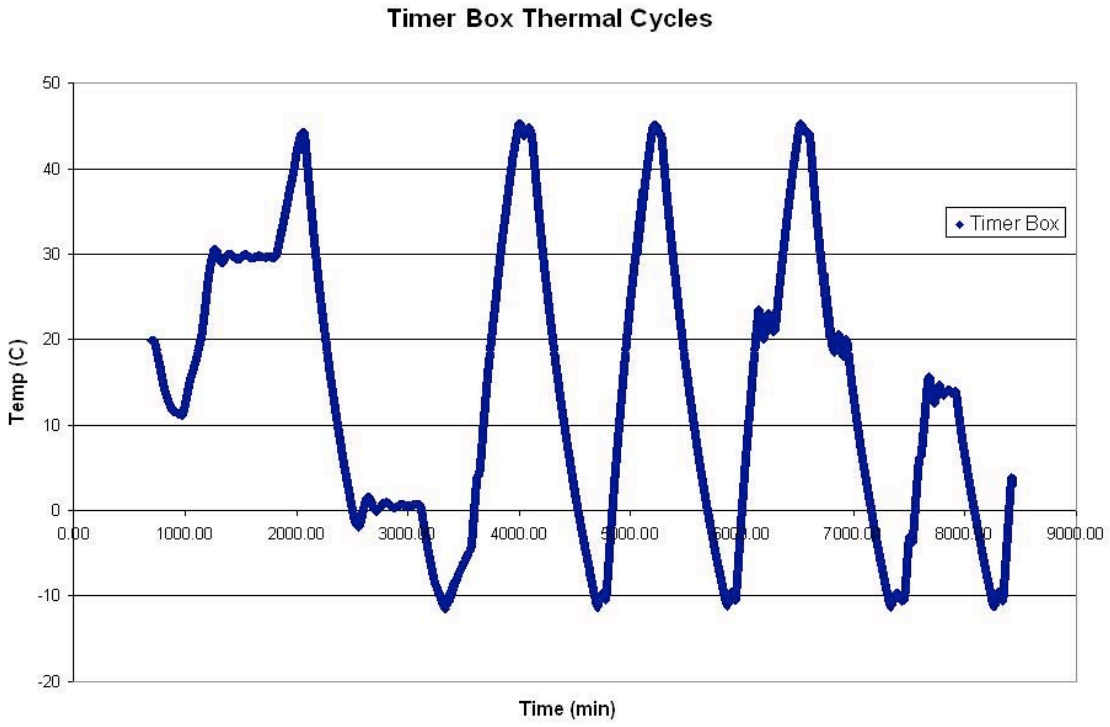

Figure 24 - Timer Box Temperature Graph

5.8.6 LCT2

The cold raw operating temperature limit for the LCT2 is -24°C. The thermal model predicted a cold balance temperature of 15.0°C, and the actual cold balance temperature was 13.5°C. According to the thermal pass/fail criteria, there is 26.4°C of margin to the raw operating temperature limit.

The hot raw operating temperature limit for the LCT2 is 65°C. The thermal model predicted a hot balance temperature of 47.2°C, and the actual hot balance temperature was 41.5°C. According to the thermal pass/fail criteria, there is 24.0°C of margin to the raw operating temperature limit.

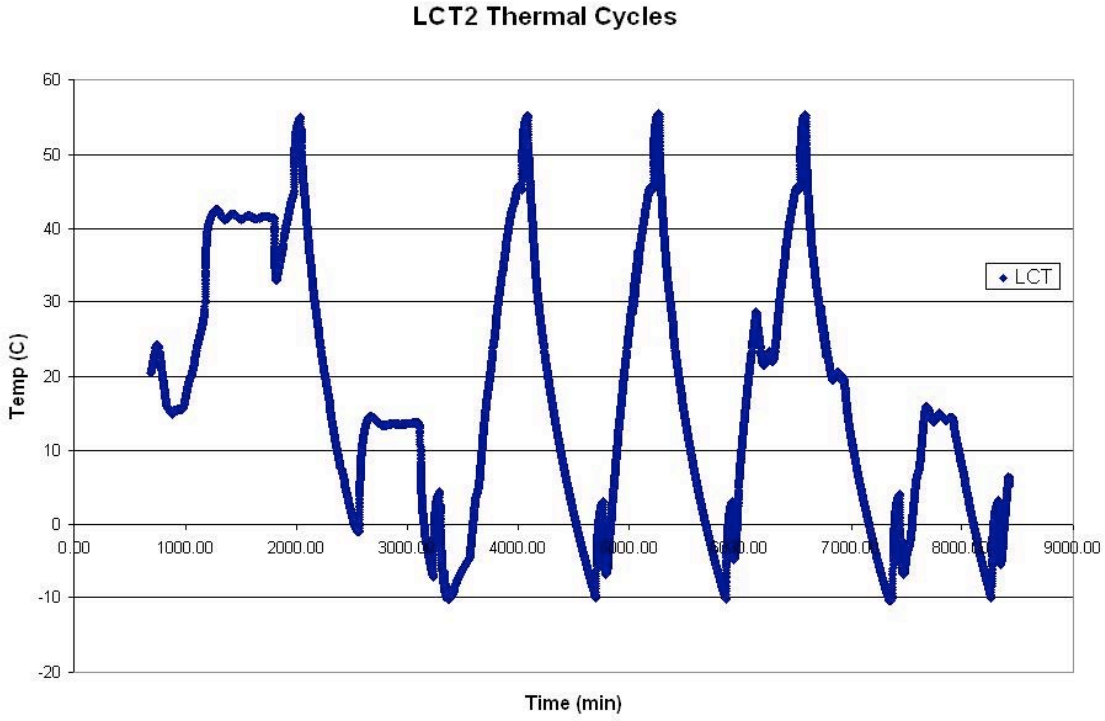

Figure 25 - LCT2 Temperature Graph

5.8.7 LCTE

The cold raw operating temperature limit for the LCTE is -20°C. The thermal model predicted a cold balance temperature of 13.5°C, and the actual cold balance temperature was 9.8°C. According to the thermal pass/fail criteria, there is 20.1°C of margin to the raw operating temperature limit.

The hot raw operating temperature limit for the LCTE is 75°C. The thermal model predicted a hot balance temperature of 45.7°C, and the actual hot balance temperature was 37.8°C. According to the thermal pass/fail criteria, there is 38.6°C of margin to the raw operating temperature limit.

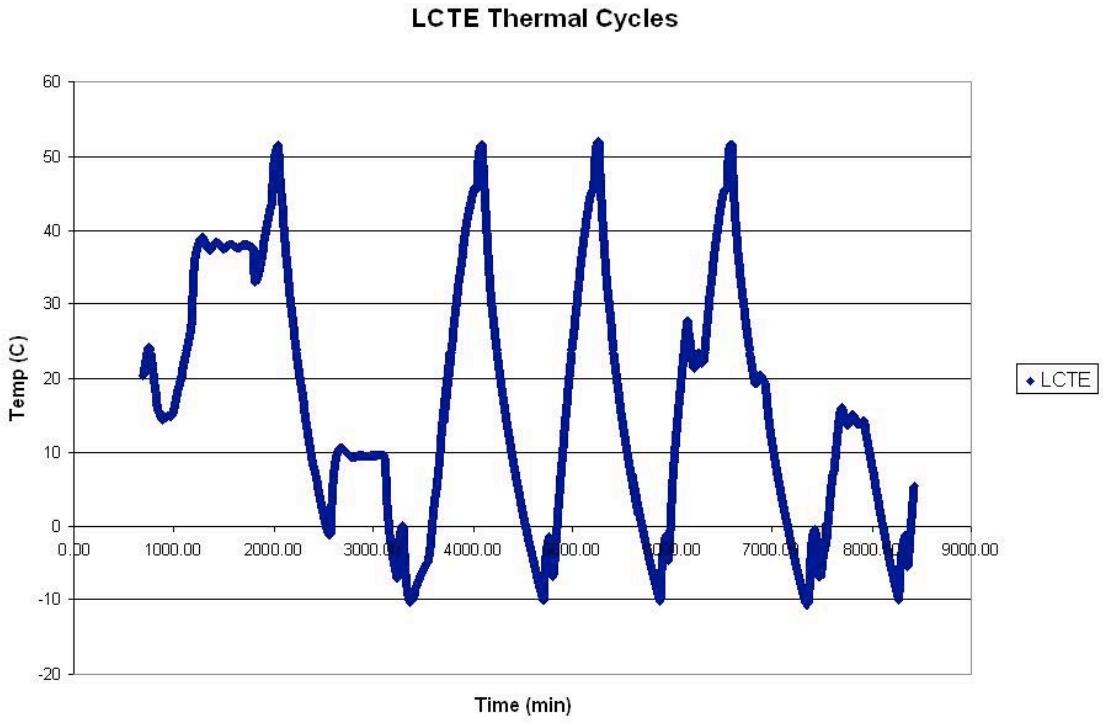

Figure 26 - LCTE Temperature Graph

5.8.8 MPE Battery Box

The cold raw operating temperature limit for the MPE Battery Box is -20°C. The thermal model predicted a cold balance temperature of 0.2°C, and the actual cold balance temperature was 0.5°C. According to the thermal pass/fail criteria, there is 27.1°C of margin to the raw operating temperature limit.

The hot raw operating temperature limit for the MPE Battery Box is 60°C. The thermal model predicted a hot balance temperature of 44.1°C, and the actual hot balance temperature was 30.8°C. According to the thermal pass/fail criteria, there is 36.1°C of margin to the raw operating temperature limit.

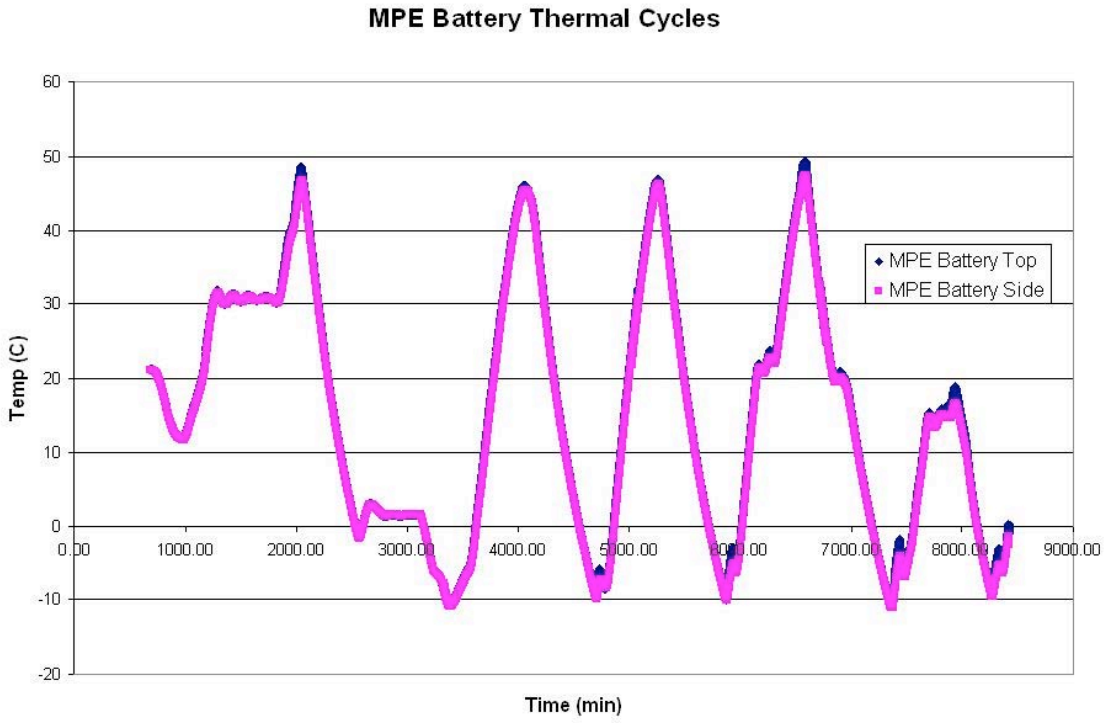

Figure 27 - MPE Battery Temperature Graph

5.8.9 Rate Sensors

The cold raw operating temperature limit for the Rate Sensors is -40°C. The thermal model predicted a cold balance temperature of 10.0°C, and the actual cold balance temperature was 10.0°C. According to the thermal pass/fail criteria, there is 44.1°C of margin to the raw operating temperature limit.

The hot raw operating temperature limit for the Rate Sensors is 80°C. The thermal model predicted a hot balance temperature of 42.3°C, and the actual hot balance temperature was 37.5°C. According to the thermal pass/fail criteria, there is 44.0°C of margin to the raw operating temperature limit.

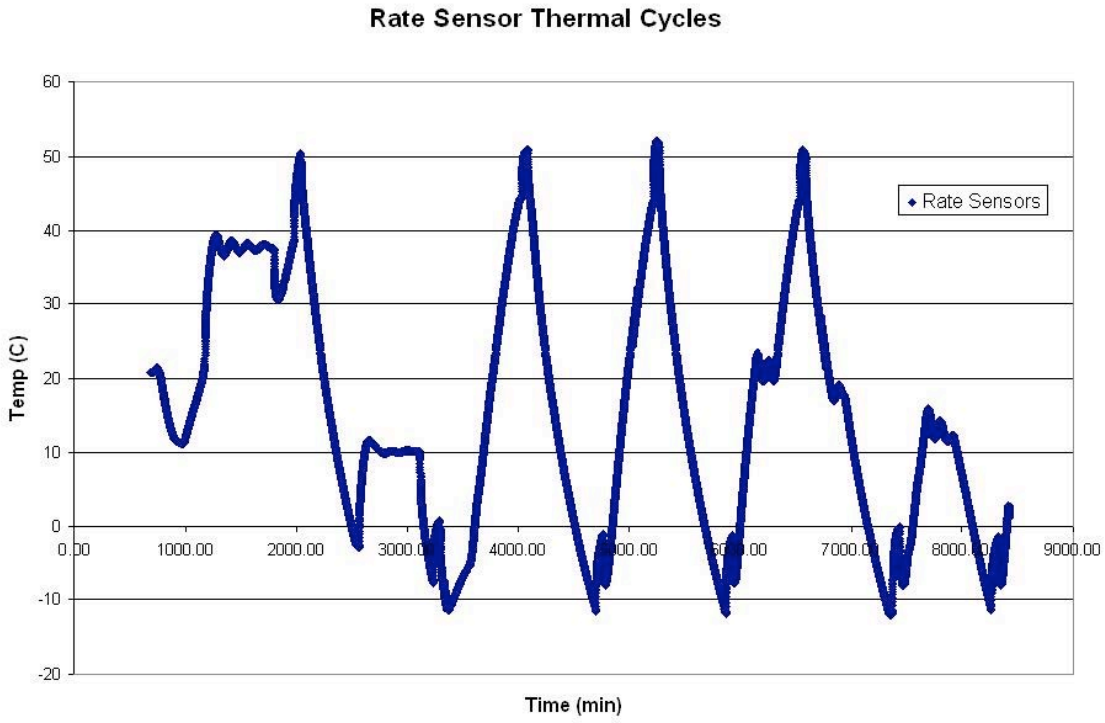

Figure 28 - Rate Sensors Temperature Graph

5.8.10 Telemetry Monitor Box

The cold raw operating temperature limit for the Telemetry Monitor Box is -20°C. The thermal model predicted a cold balance temperature of 1.5°C, and the actual cold balance temperature was 4.0°C. According to the thermal pass/fail criteria, there is 26.8°C of margin to the raw operating temperature limit.

The hot raw operating temperature limit for the Telemetry Monitor Box is 85°C. The thermal model predicted a hot balance temperature of 41.9°C, and the actual hot balance temperature was 33.3°C. According to the thermal pass/fail criteria, there is 56.8°C of margin to the raw operating temperature limit.

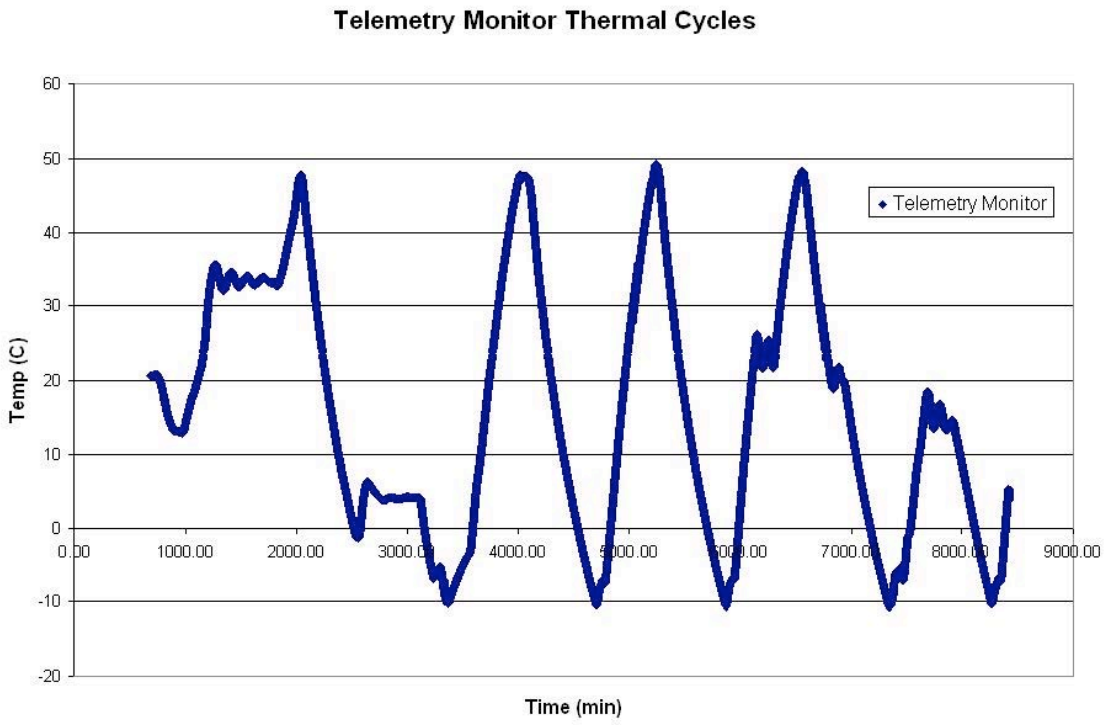

Figure 29 - Telemetry Monitor Temperature Graph

5.9 CONCLUSION: QUALIFICATION TEST SUCCESS CRITERIA

The success criteria for the MPE thermal system are:

- Criteria #1: When the difference between measured and predicted temperatures for thermal balance is added to flight predictions, there is positive margin for all avionics systems with respect to the raw component limit.
    - Based on the results from the thermal balance test, MPE demonstrates positive margins for both worst case hot and cold scenarios.
- Criteria #2: All MPE components operate nominally after completion of thermal vacuum cycle testing

- Based on the results from the thermal vacuum cycle testing, MPE has demonstrated all components operated successfully over the qualification temperature range.

6. FUTURE WORK

6.1 STORAGE AND POST HIBERNATION PLAN

After successful completion of the thermal qualification program, MPE was placed into storage until a flight opportunity has been identified by NASA. All MPE disciplines created a hibernation plan and subsequent flight preparation plan, to place MPE into a safe state for storage and perform any remaining tasks once MPE comes out of hibernation. The thermal discipline has the following tasks to complete once MPE is out of hibernation.

- Inspect all MLI blankets, silver Teflon tape, and VDA Kapton for integrity and no degradation
- Clean thermal flight hardware to Class 100,000 cleanroom or higher requirements
  - There shall be no fingerprints or foreign substances on thermal hardware
- Replace any thermal flight hardware if damage has occurred
  - For example, lift points and payload interface plates
- Confirm Planetary Systems Corporation Lightband temperature qualification limits
- Flight MLI blankets shall be closed out with 2nd surface 2 mil VDA Kapton, grounded to the MPE structurem and vents exposed

- Thermal Model Updates
    - Obtain thermal models or geometries of flight payloads and incorporate into the overall MPE flight model
    - Perform final thermal analysis with flight payload models
    - Verify MPE avionics temperature limits are not exceeded

7. APPENDIX A – HOT THERMAL BALANCE DATA

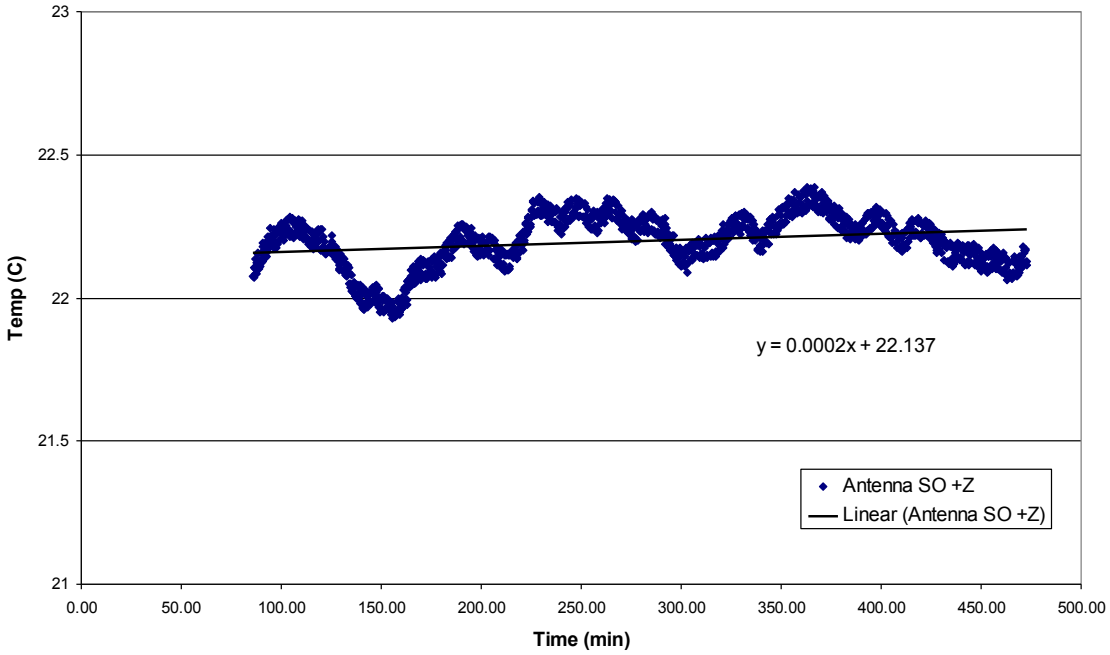

Figure 30 - +Z Antenna Hot Balance

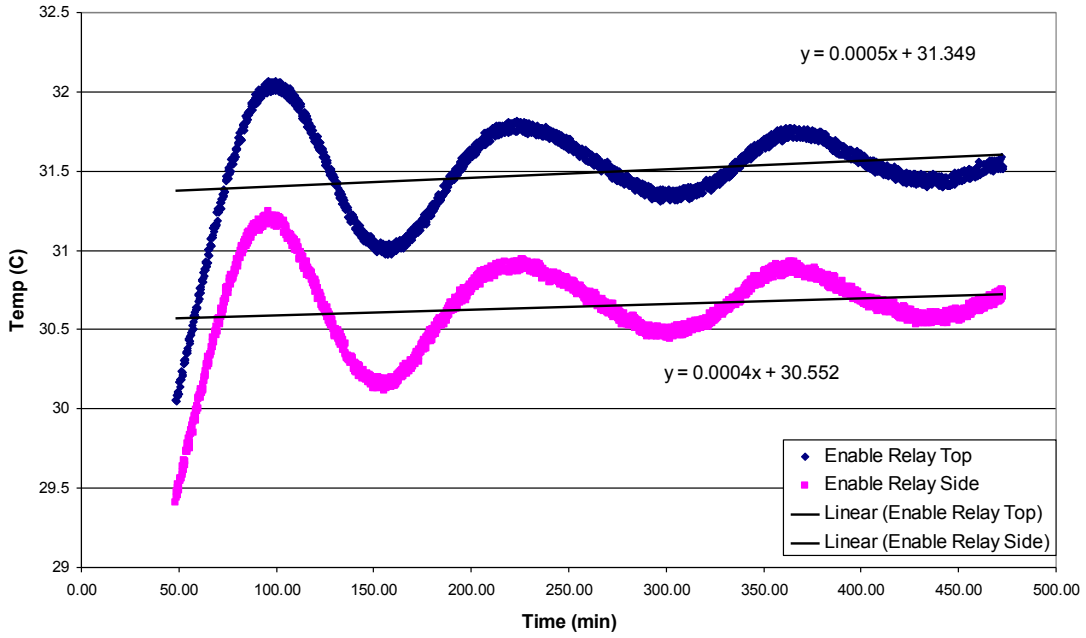

Figure 31 - Enable Relay Box Hot Balance

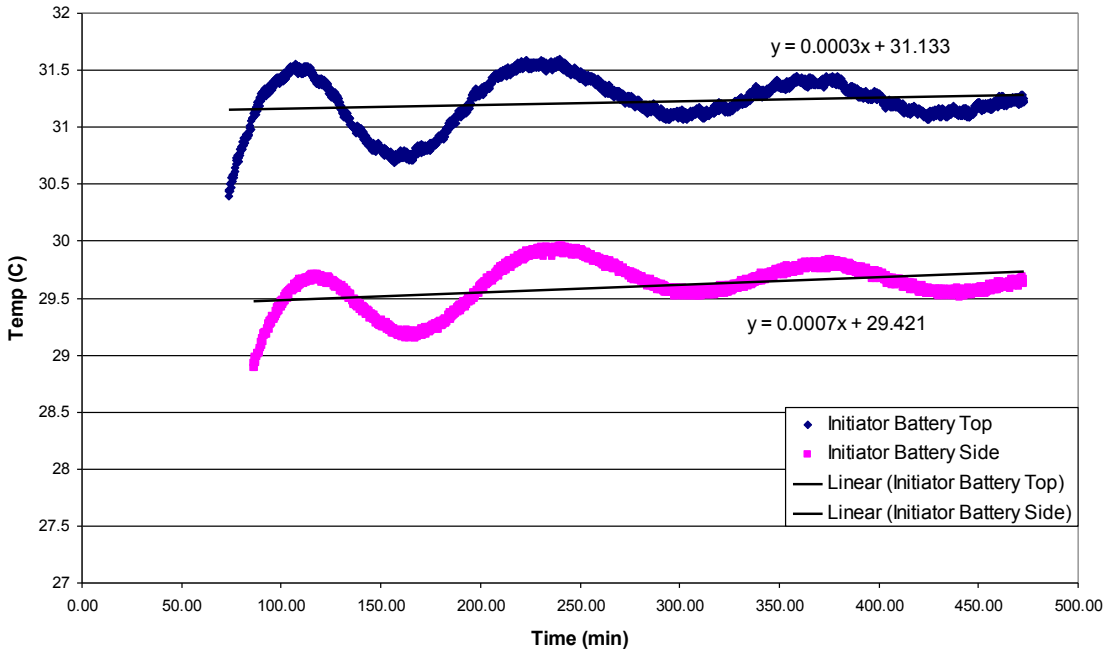

Figure 32 - Initiator Battery Hot Balance

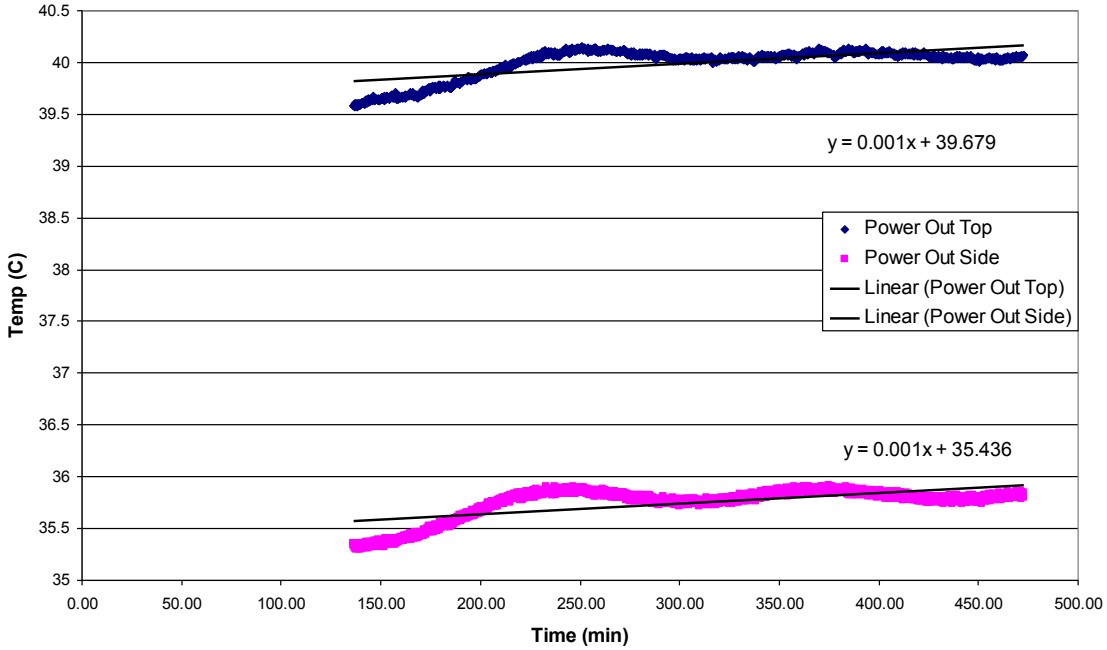

Figure 33 - Power Out Hot Balance

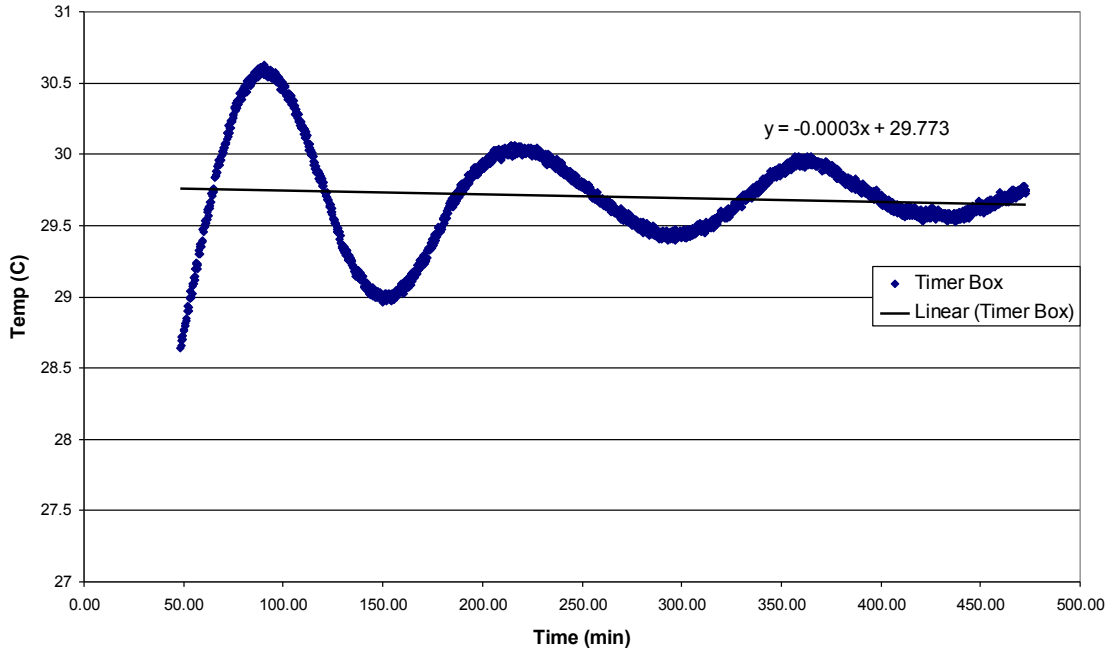

Figure 34 - Timer Box Hot Balance

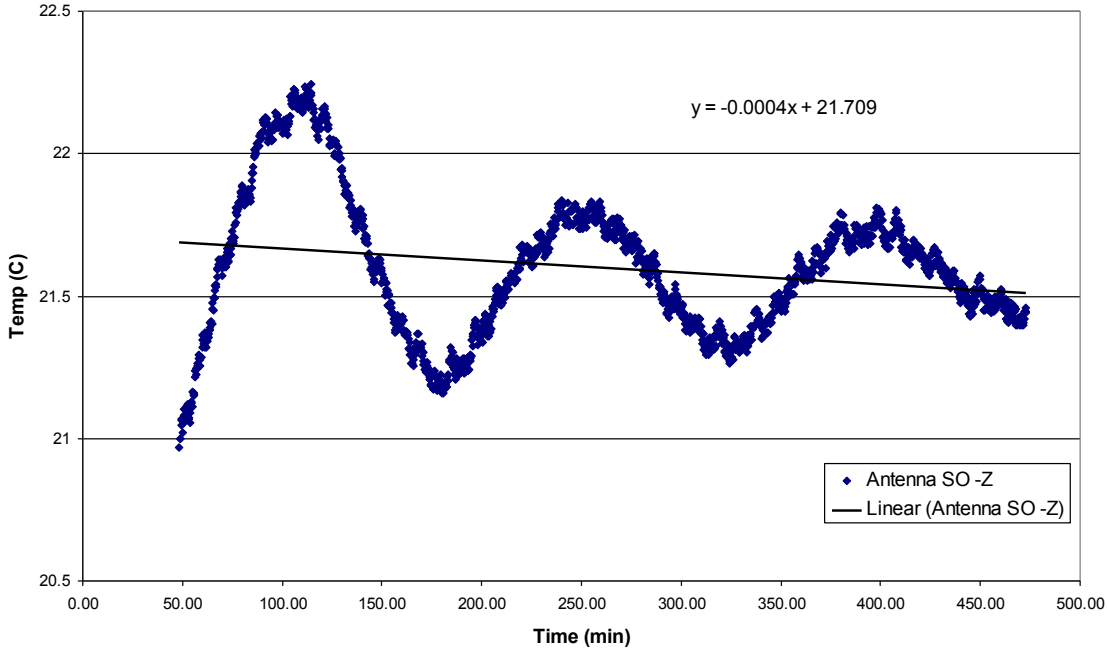

Figure 35 - -Z Antenna Hot Balance

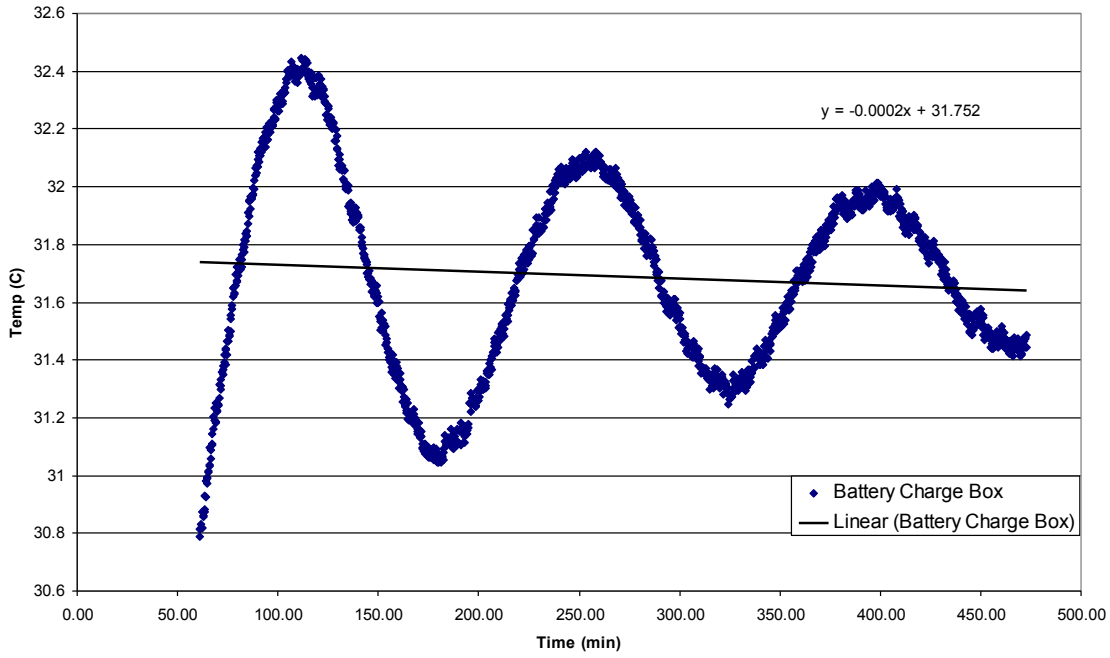

Figure 36 - Battery Charge and Monitor Box Hot Balance

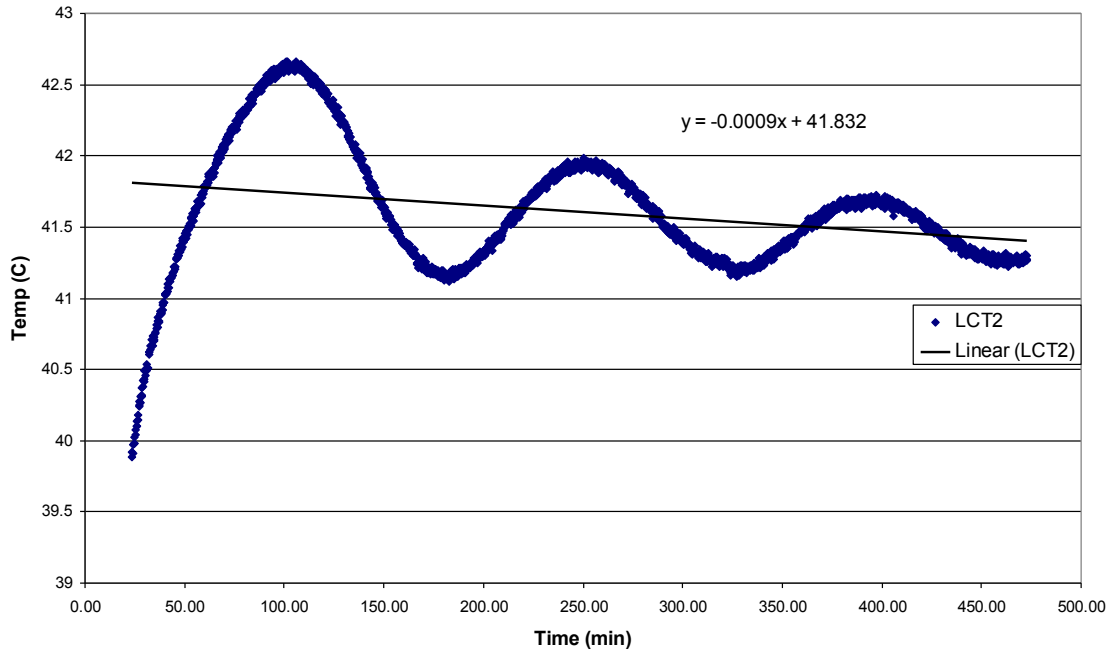

Figure 37 - LCT2 Hot Balance

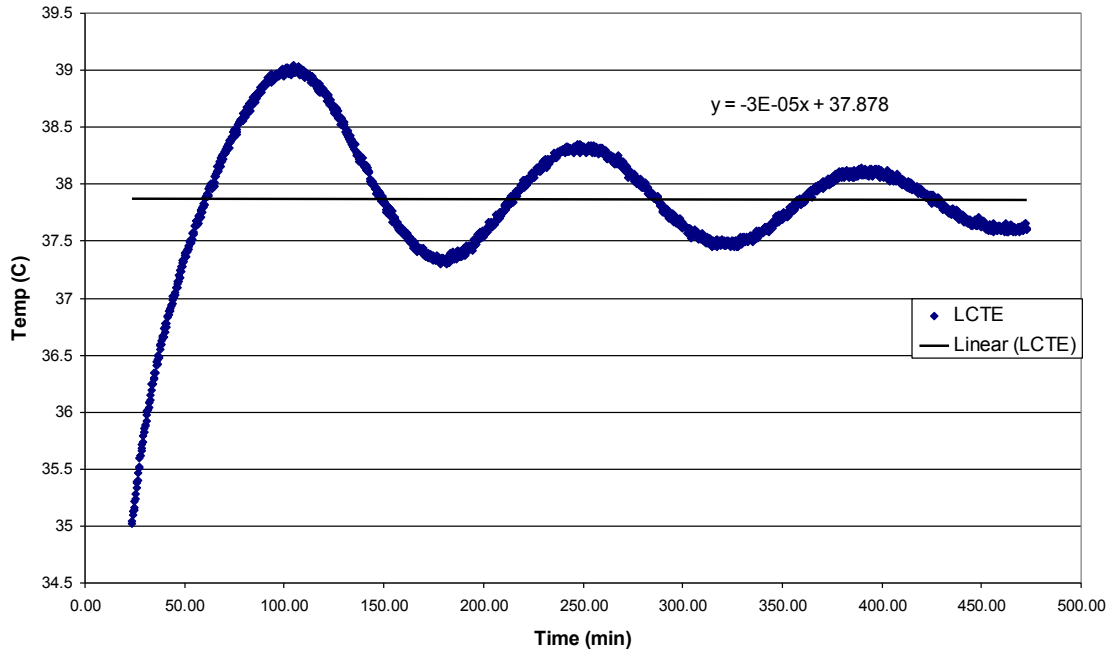

Figure 38 - LCTE Hot Balance

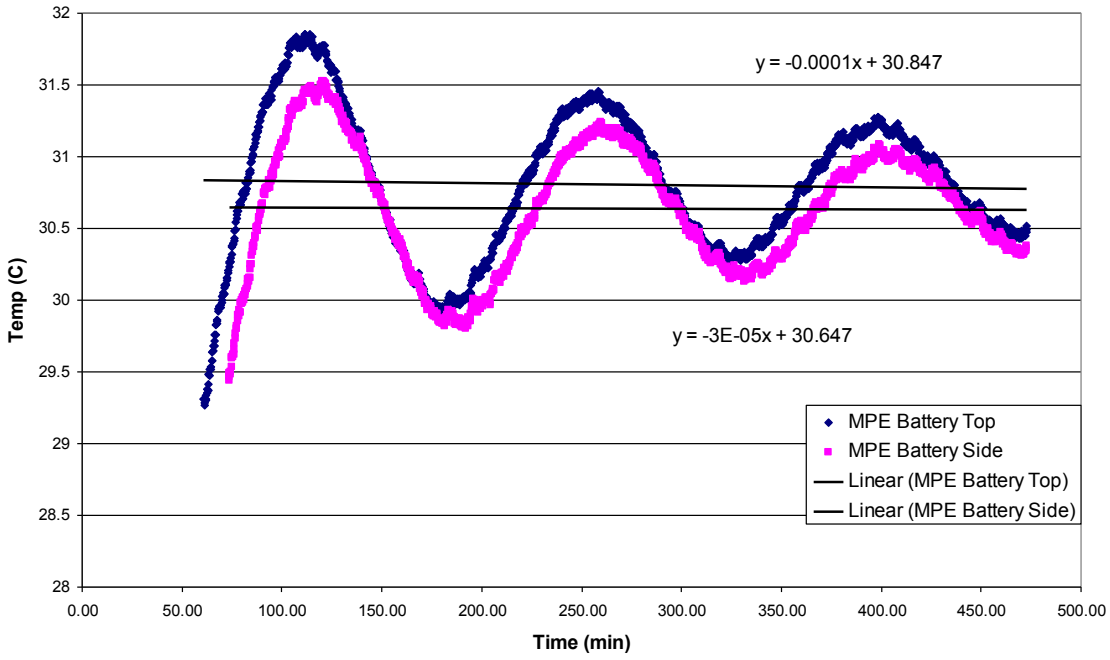

Figure 39 - MPE Battery Hot Balance

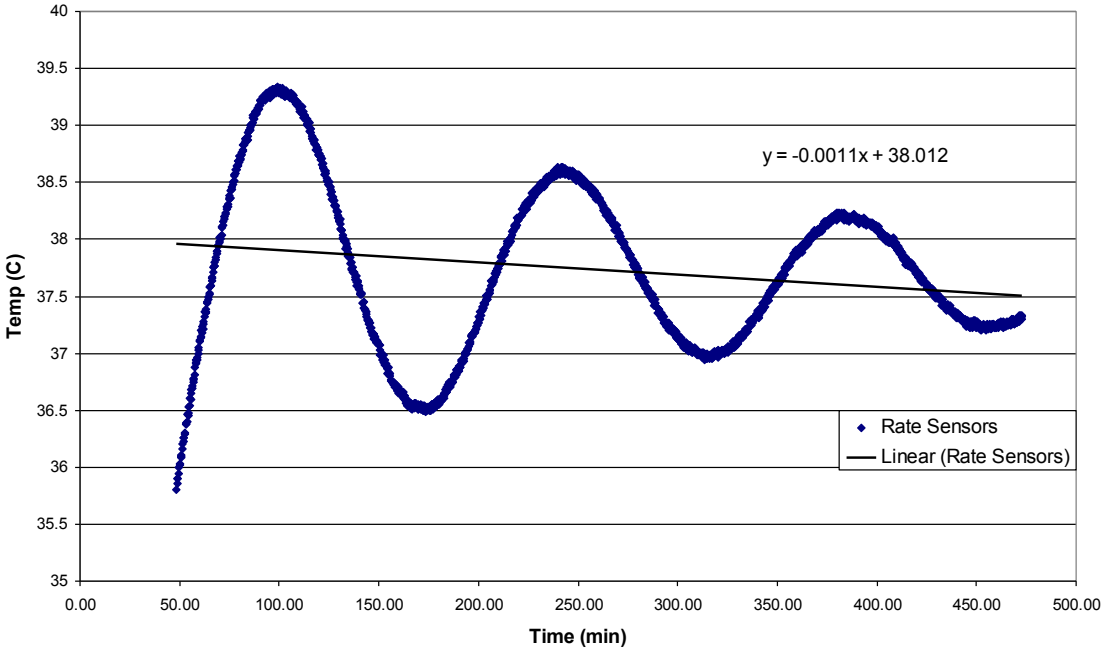

Figure 40 - Rate Sensors Hot Balance

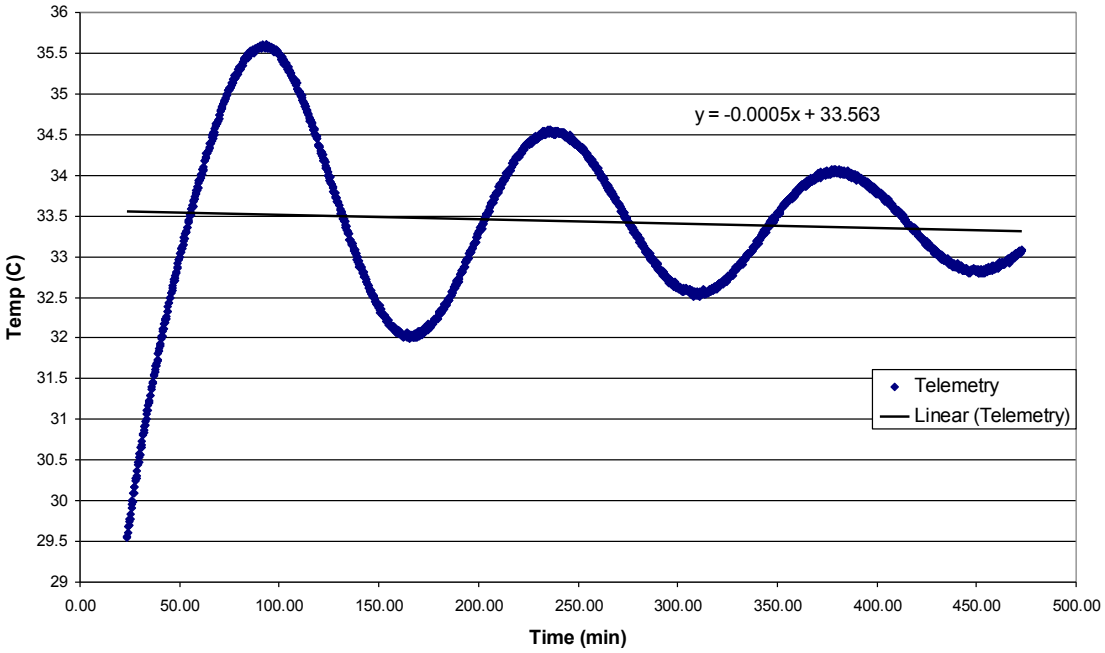

Figure 41 - Telemetry Monitor Box Hot Balance

8. APPENDIX B – COLD THERMAL BALANCE DATA

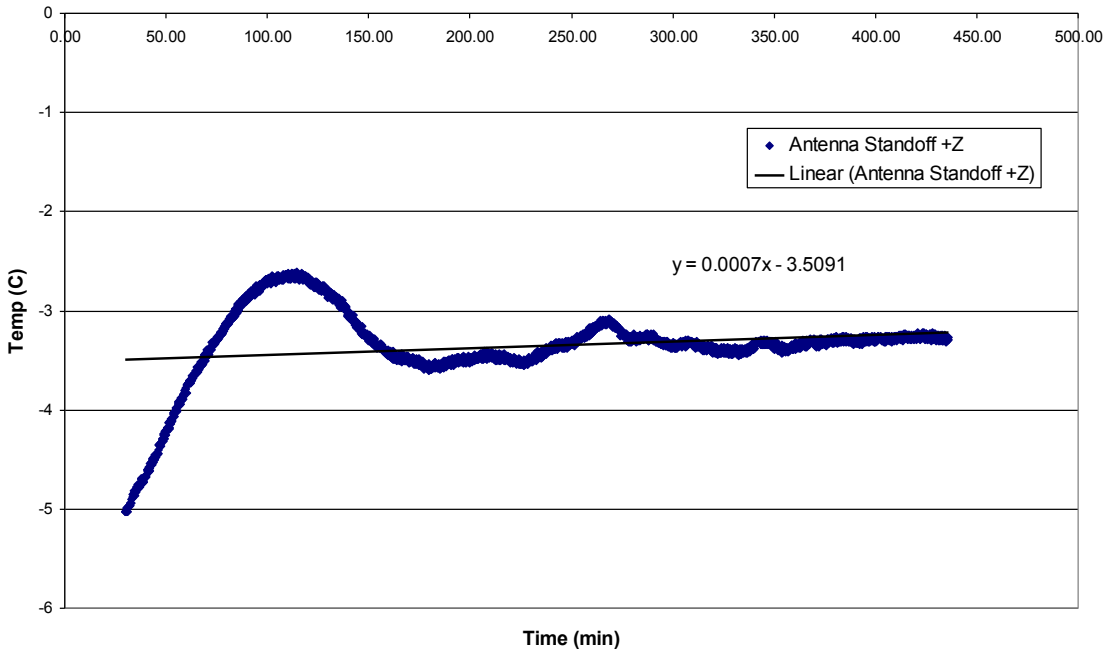

Figure 42 - +Z Antenna Cold Balance

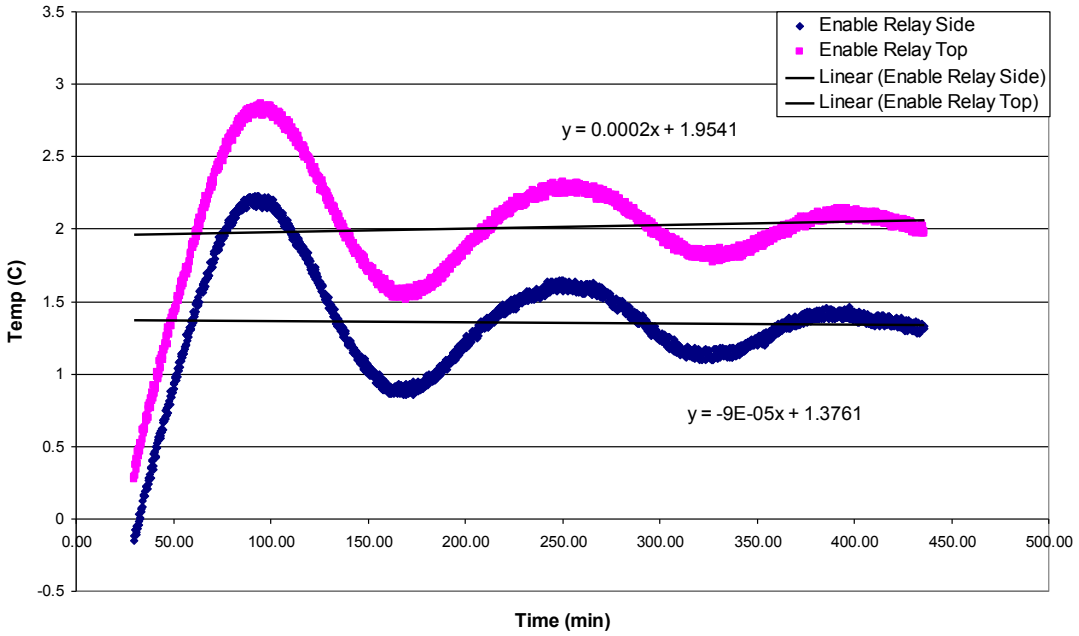

Figure 43 - Enable Relay Box Cold Balance

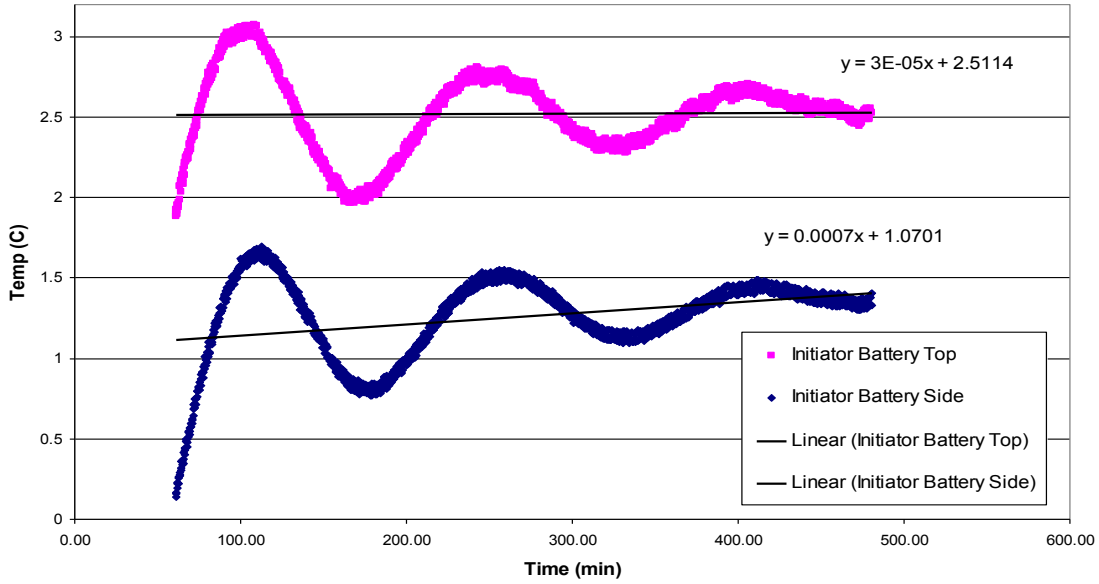

Figure 44 - Initiator Battery Cold Balance

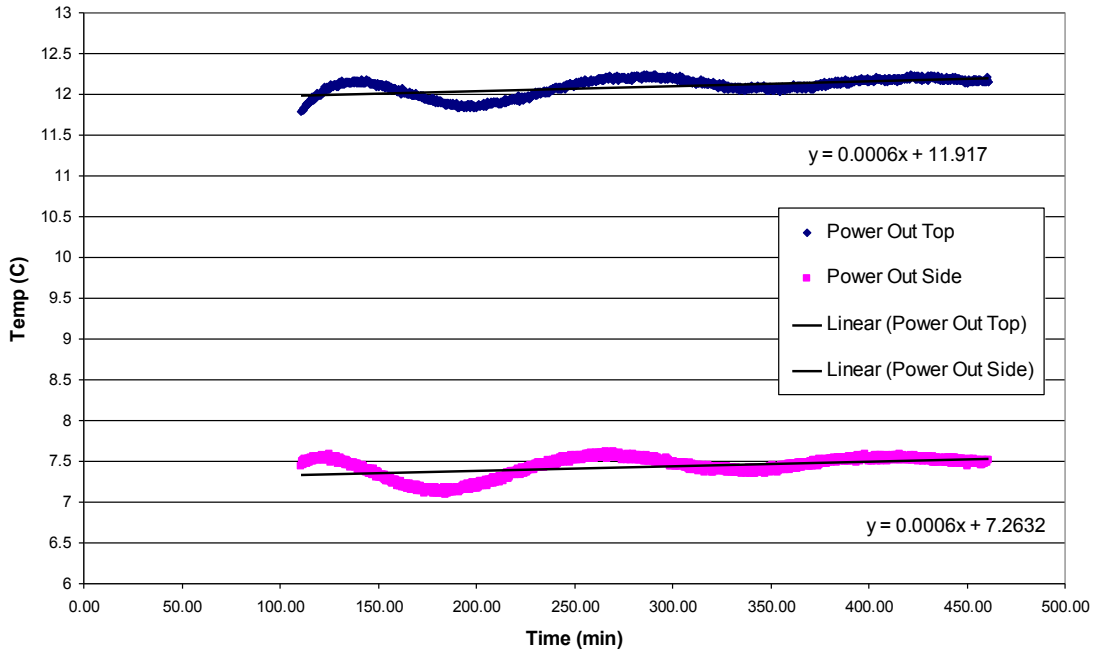

Figure 45 - Power Out Box Cold Balance

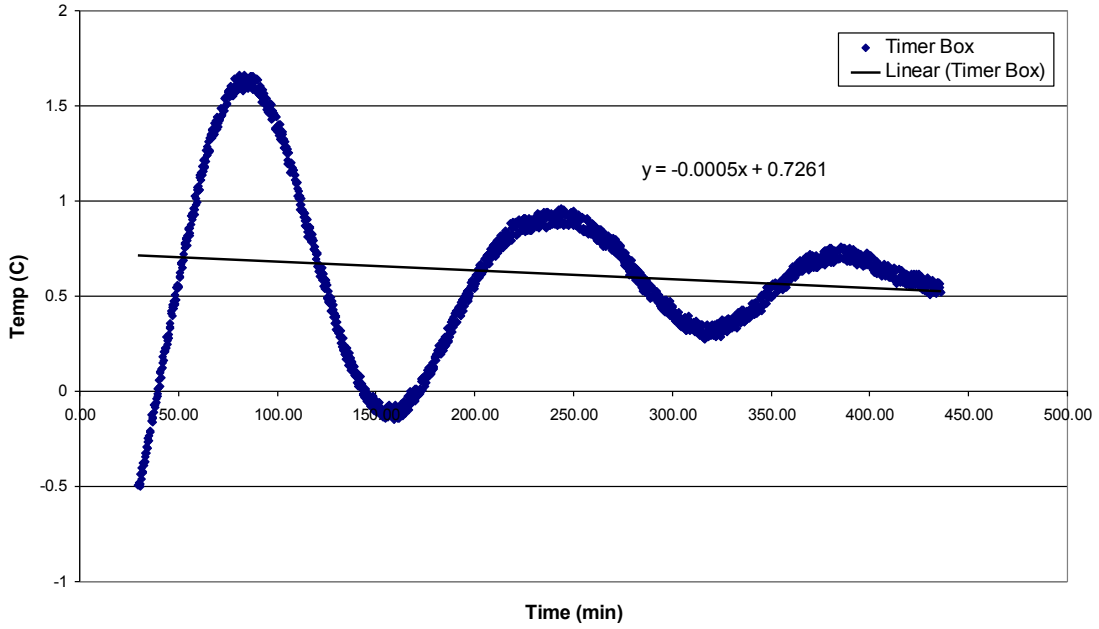

Figure 46 - Timer Box Cold Balance

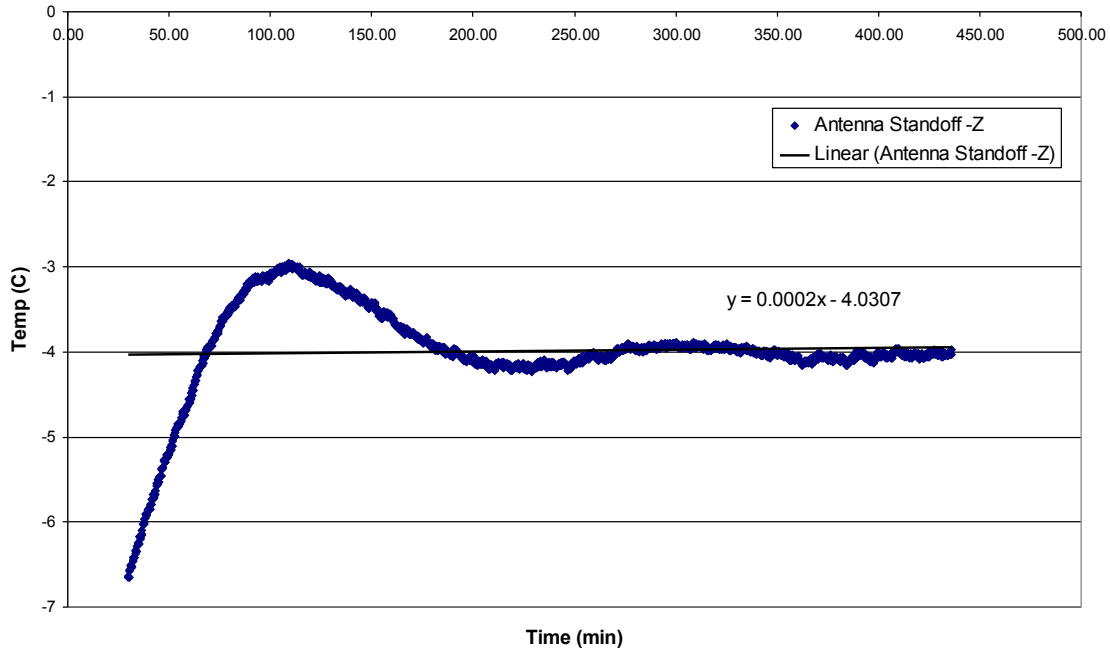

Figure 47 - -Z Antenna Cold Balance

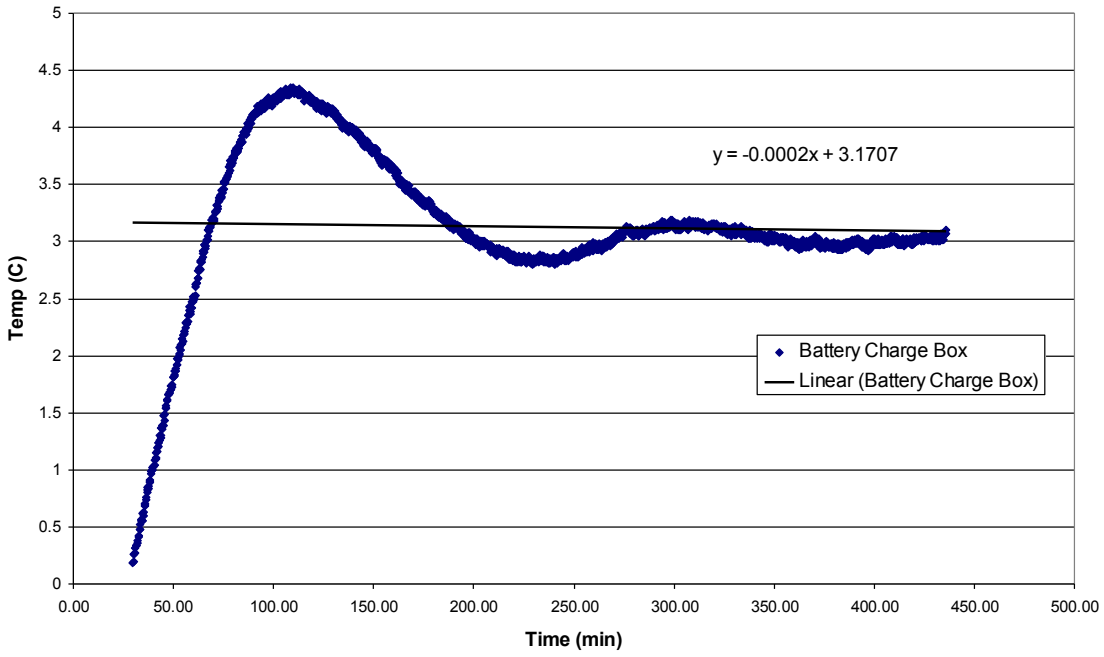

Figure 48 - Battery Charge and Monitor Box Cold Balance

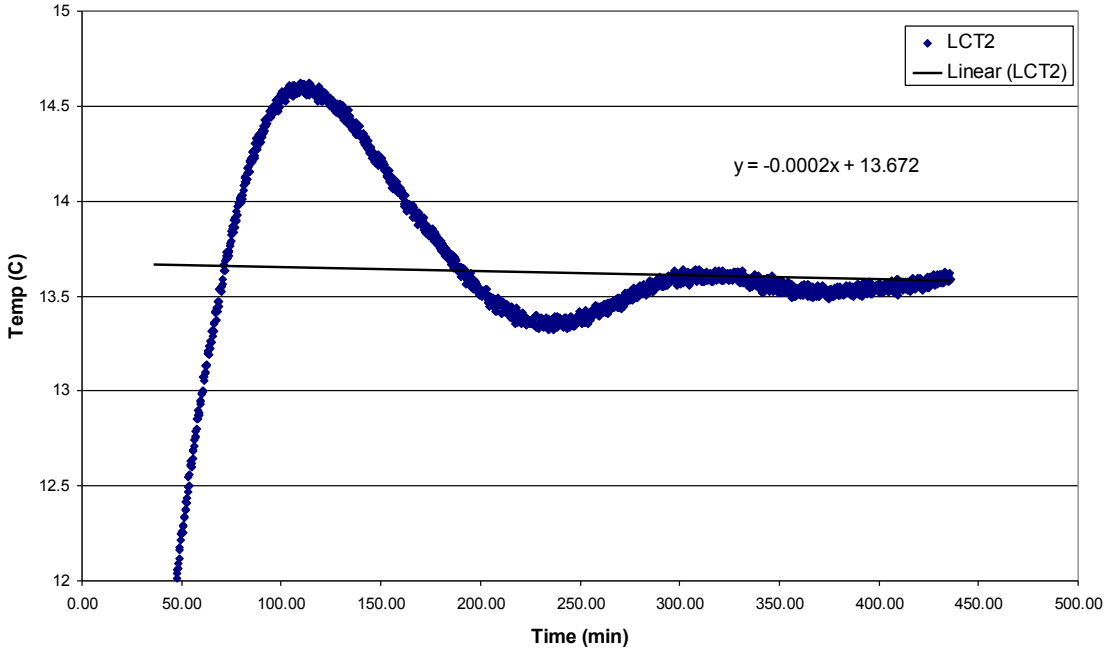

Figure 49 - LCT2 Cold Balance

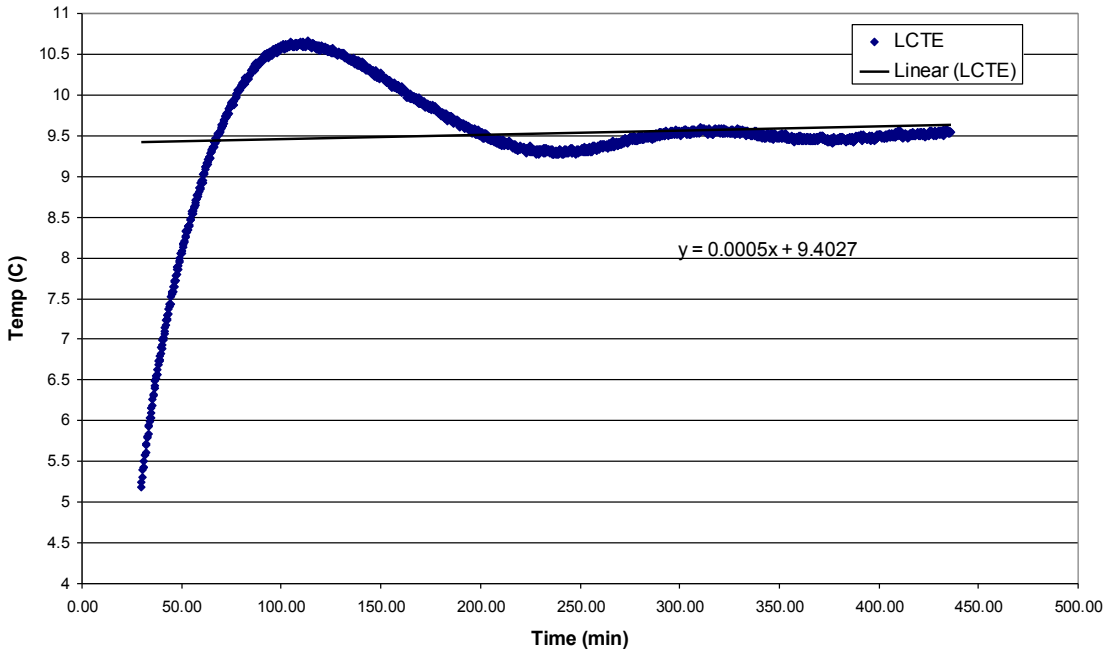

Figure 50 - LCTE Cold Balance

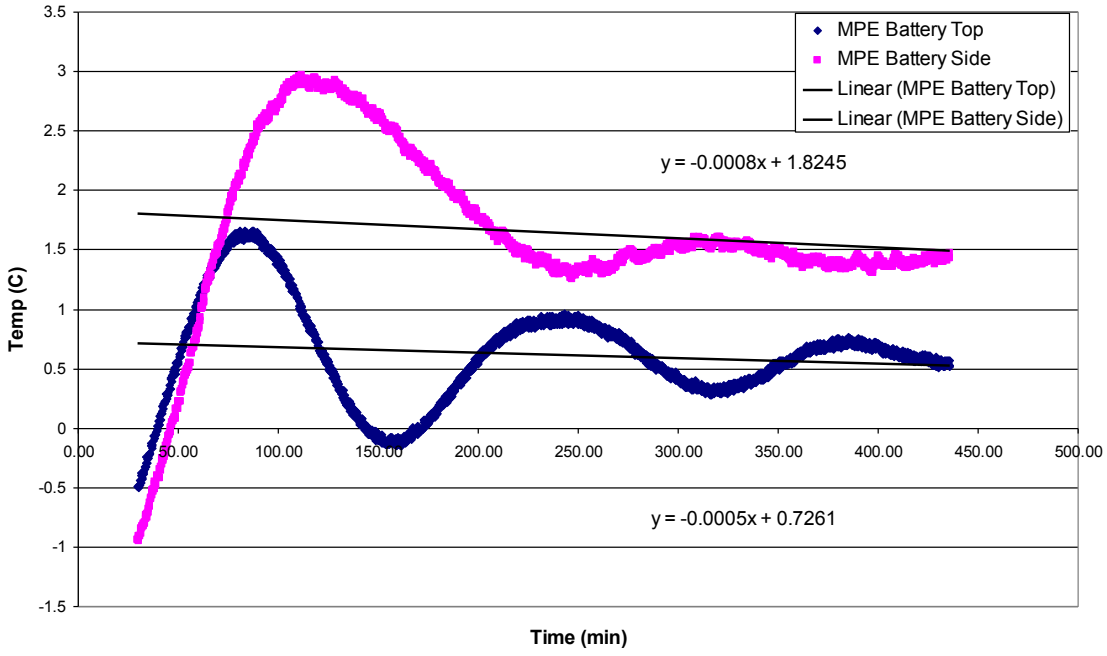

Figure 51 - MPE Battery Cold Balance

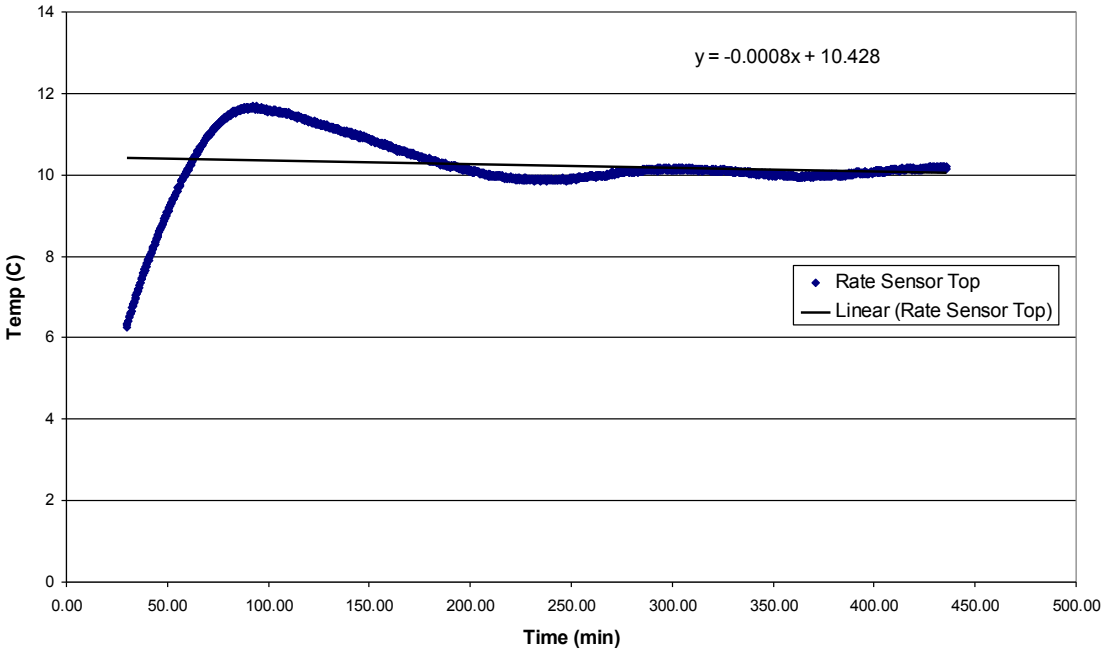

Figure 52 - Rate Sensor Cold Balance

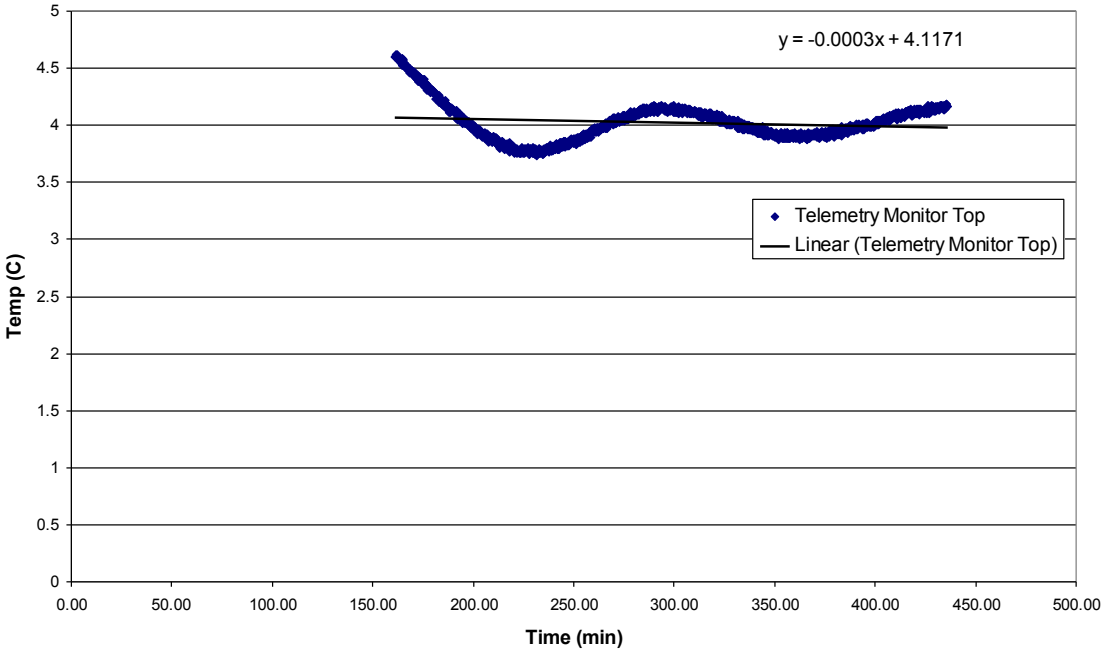

Figure 53 - Telemetry Monitor Box Cold Balance

9. APPENDIX C – AS-RUN MPE TVAC TEST PLAN AND PROCEDURES AND ASSOCIATED TEST LOGS

This Appendix C contains the following As-Run procedure documents and associated test data logs below:

1. The MPE System Qualification TVAC As-Run Test Plan and Procedures, 802-PROC-0003
2. The MPE TVAC Thermal Test Engineers Log
3. The MPE TVAC Chamber Operator Log
4. The MPE TVAC Harrel Heater Rack Setpoints
5. The MPE TVAC Logbook with documented observations

9.1 APPLICABLE DOCUMENTS

9.1.1 Reference Documents

GEVS-STD-7000	General Environmental Verification Specification

9.1.2 Project Documents

802-PROC-0003	MPE System Thermal Vacuum Test Plan and Procedure
802-PROC-0049	MPE Limited Performance Test Procedure

9.1.3 Facility Documents

SAIWFF-PROC-001	Operating Procedure for the Wallops Flight Facility Thermal Vacuum Chamber

SAIWFF-PROC-002	Wallops Flight Facility Thermal Vacuum Chamber Equipment Failure, Power Outage, and Other Emergencies Procedure
SAIWFF-PROC-003	Operating Procedure for the Harrel Heater Rack